• U C •

FCTUC FACULDADE DE CIÊNCIAS
E TECNOLOGIA
UNIVERSIDADE DE COIMBRA

Daniel Faustino de Noronha Osório

Modeling Physiological Systems - A computational and hybrid approach

Dissertação apresentada à Universidade de Coimbra para cumprimento dos requisitos necessários à obtenção do grau de Mestre em Engenharia Biomédica

Thesis submitted to the University of Coimbra in compliance with the requisites for the degree of Master in Biomedical Engineering

Supervisors:

Professor Alberto Cardoso
Professor César Teixeira

Coimbra, 2015

This thesis was developed in collaboration with:

Centro de Informática e Sistemas da Universidade de Coimbra

Acknowledgment

In the last years there have been many people who have have been key to for my success and happiness.

My first words of gratitude go to my supervisor, Professor Doctor Alberto Cardoso, and my co-supervisor, Professor Doctor César Teixeira. They have helped me through out the past year, with their guidance and support, providing a pleasant and relaxed work environment.

Next I want to say thank you to my parents and my sister, for the opportunities, love and support they provided me over the years.

During my years in Coimbra I made many friends. I would like to say a special thanks to Carolina Silveira, Diogo Martins, Diogo Passadouro, Filipe Costa, Mariana Nogueira, Inês Barroso, Heloísa Sobral, Bruna Nogueira, Ricardo Simões, Luís Henriques, Rui Venâncio and João Fragoso for all the many crazy and mostly fun moments we had.

I would also want to say a special thank you to my hometown friends, many of whom study or studied in Coimbra as well, especially to Francisco Brito, Ricardo Coke, Nuno Oliveira, Francisco Seixas, Rui Eirô and Diogo Almeida.

"It is human nature to find patterns where there are none and to find skill where luck is a more likely explanation."

William J. Bernstein,
financial theorist and neurologist

"That which can be asserted without evidence, can be dismissed without evidence."

Christopher Hitchens,
author and journalist

Abstract

Mathematical models have proven to be a valuable tool in the understanding of physiological processes in the human body [1]. The intent of this thesis is the development of physiological models, both computational and hybrid.

A computer model is a representation of a system or process created on a computer, to assist calculations, predictions or/and visualizations. In this work, this type of model was used to analyse a system/make predictions.

Using a collections of several physiological variables from 7 different surgical procedures, a relation between the recorded variables (measures) and the bi-spectral index, BIS, was sought. This index can be used during surgeries to monitor the anaesthetic state of a patient, but can be very difficult to obtain or reliably be used. For this reason, an interest arise in using other measures to complement the BIS, in order to aid physicians when monitoring a patient. From the analysis performed, a correlation between some measures and the BIS was found, and using these correlation two different type of models were developed.

A hybrid model can be defined as the usage of computer models in parallel with transducers. In this thesis, a remote lab simulating the ingestion of a drug was developed and compared to a computer model for the ingestion of paracetamol.

This model was achieved by using a three-tank process, in which each tank represents a different body compartment (intestine, bloodstream or bladder). The developed model was then ported to a web interface in order to be used as a remote lab, allowing simulation of ingestions to be performed remotely and monitored using water level sensors and a camera. An off-line model was developed as well in order to provide a testing ground for users to experiment different settings. The development of this lab resulted in a demo in a conference (appendix H), an article submission to a journal and is going to be used as a teaching aid in the subject "Modelos Computacionais de Processos Fisiológicos".

Resumo

Os modelos matemáticos têm provado ser uma ferramenta valiosa para a compreensão de processos fisiológicos do organismo humano [1]. O objetivo desta tese foi o desenvolvimento de modelos fisiológicos, tanto computacionais como híbridos.

Um modelo computacional é uma representação de um sistema ou processo criada em computador, como auxílio ao cálculo, à previsão e/ou visualização dos mesmos. Nesta tese estes modelos foram usados para analisar um sistema e fazer previsões.

Usando uma coleção de diversas variáveis fisiológicas de 7 procedimentos cirúrgicos diferentes, foi pesquisada uma relação entre as variáveis recolhidas e o índice bi-espetral (BIS). Este índice pode ser utilizado durante cirurgias para monitorizar o estado anestésico de um paciente, mas pode ser muito difícil de obter ou de ser utilizado com segurança. Por esta razão, houve interesse em utilizar outras variáveis para complementar o BIS, a fim de auxiliar os médicos durante a monitorização de um paciente. A partir da análise efetuada, foi encontrada uma correlação entre algumas das variáveis e o BIS, e apartir desta correlação dois tipos diferentes de modelos foram desenvolvidos.

O modelo híbrido pode ser definido como um modelo que combina transdutores e instrumentos com um modelo de computador para estudar ou simular um processo. O modelo desenvolvido simula a ingestão, propagação e excreção de um fármaco no corpo humano, neste caso o paracetamol.

Este modelo foi conseguido usando um processo de três tanques, em que cada tanque representa um compartimento diferente do corpo (intestino, corrente sanguínea ou bexiga). O modelo desenvolvido foi adaptado para uma interface web, a fim de ser utilizado como um laboratório remoto, permitindo que se executem remotamente simulações de ingestões e estas possam ser monitorizadas por meio de sensores nos tanques e uma câmara de video. Foi também desenvolvido um modelo off-line, a fim de proporcionar uma área de testes para os utilizadores experimentarem diferentes configurações. Do desenvolvimento deste laboratório resultou uma demonstração numa conferência (apêndice H), uma submissão de um artigo para uma revista da área e irá ser usado como um auxiliar no ensino da disciplina "Modelos Computacionais de Processos Fisiológicos".

List of Tables

List of Figures

Contents

Chapter 1

Introduction

This project was developed in the Department of Informatics Engineering (DEI) of the Faculty of Sciences and Technology of the University of Coimbra (FCTUC), within the Biomedical Engineering Masters program.

1.1 Motivation

Mathematical models have proven to be a valuable tool for the understanding of physiological processes in the human body [1]. As modelling techniques evolve in academia, porting such techniques onto real-life applications is a very appealing proposition. They can be used in different contexts, from helping physicians to establish a diagnosis, discover previous unknown patterns and relations, predict the behaviour of an action or in a teaching environment.

In other engineering fields, such as mechanical or electrical engineering, modelling is a common practice and with the surfacing of powerful computer systems in recent time, is getting increasing popularity. In recent years, three major areas of influence were found where mathematical modelling finds application in a physiological environment: medical research, education and supporting clinical practices [10], especially in the pharmaceutical R&D where silicio studies and trial simulations complement experimental approaches [11], or medical simulation (a brief history starting in 1938 can be found in [12]).

1.2 Objectives

The main objective of this thesis was the building of physiological models, both computational and hybrid (a mixture of computer based controllers and real world equipment).

A computer model is a representation of a system or process created on a computer, to assist calculations, predictions or/and visualizations. In this work, this type of model was used to analyse a system/ make predictions.

In the development of a computer model, a dataset made up by a set of 43 biomedical measures recorded during surgery of seven different patients, in a collaboration between the Anaesthesiology Department of the of Centro Hospitalar e Universitário de Coimbra (CHUC) and the Centre for Informatics and Systems (CISUC) of the Department of Informatics Engineering of the University of Coimbra.

Based upon other studies and research and an interest to use available data from real patients, an idea of constructing a model that could predict the anesthetic state of a given patient by modeling the bi-spectral index, BIS, arose. An insight about this variable is given in the beginning of chapter 4. The main objective was the development of a model that uses the input of four different variables to make a prediction about the BIS.

A hybrid model can be defined as the usage of computer models in parallel with transducers. In this thesis, a remote lab simulating the ingestion of a drug was developed and compared to a computer model for the ingestion of paracetamol.

The objective of building a hybrid remote lab in this thesis context was to provide a platform where the intake, propagation and excretion of a drug can be simulated and viewed remotely. In conjunction with the online hybrid model, an offline simulation of the process was developed.

By being a remote lab, the simulation and the model can be used in a teaching environment, to explain what is an equivalent model and how can one be developed.

The remote lab experiment was used as a demonstration at Experiment@ Portugal International Conference in Azores (exp.at'15), where the process was remotely controlled [13] (appendix H). An article will also be submitted to the International Journal of Online Engineering (iJOE) [14]. This lab will also be used during the subject "Modelos Computacionais de Processos Fisiológicos" as a teaching aid.

In summary, the objectives of this thesis were the development of a BIS predictor based on other recorded variables and the development of a drug ingestion model adapted into a three-tank system integrated in a remote lab environment.

1.3 Planning

Figure 1.1 presents the time spent for each stage of this thesis. For each major stage there is a brief description of the work done.

1.3.1 Literature review

The state-of-the-art was developed during the first semester. Included in the knowledge discovery period are the meetings with physicians from Internal Medicine A of the CHUC. The purpose of these meetings was to query the units physicians about possible questions to be answered in line with this thesis.

During this period, different physiological systems were study in order to find the most suitable in this context.

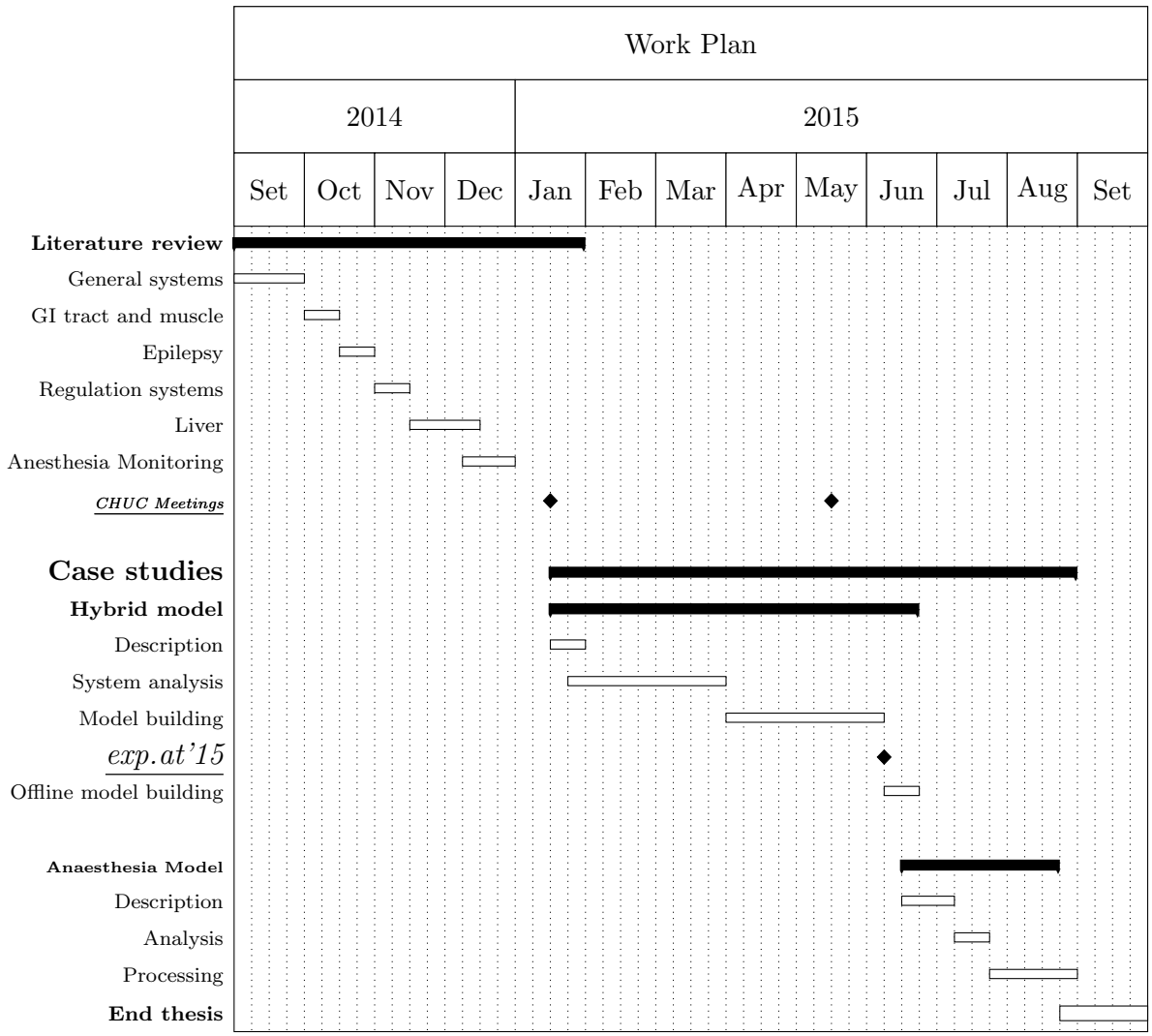

Figure 1.1: Gantt chart representing the work plan.

1.3.2 Case studies

Hybrid model

The first of the two models developed was the hybrid model, due to a hard deadline for submission and presentation of this model at the exp.at'15 conference. During this period, research was done about other case studies using remote labs, control models, system limitations and capabilities and alternative models. At the same time, the platform used to access and send control values to the tank pumps was being developed by Vitor Sousa in the context of his master thesis [15]. After exp.at'15, an offline model was also developed.

During several discussions on what hybrid model should be developed based on the state of the art, the possibility of using a remote lab to model and simulate a drug ingestion, propagation and excretion surfaced was a good choice.

To achieve this objective, a three-tank process, coupled with two voltage controlled pumps, an ADC/DAC controller interface, a computer controlling the process and an IP webcam were used. Also, a web interface that allows the simulation of a drug ingestion in 'real time'[1] and monitor the water tank reaction, was developed, as well as an offline simulation in order to compare the results obtained by the online model and, if the remote lab cannot be accessed, be a replacement of it.

The online model was showcased at exp.at'15 conference in Azores (appendix H), will be used as a teaching aid and an article will also be submitted to the International Journal of Online Engineering (iJOE) [14].

Computational model

A common metric to assess a patient level of anaesthesia is the BIS. One of the main problems encountered when using the BIS[2] was missing values. One of the reasons that can explain these missing values is the interference caused by the electric scalpel or a low signal quality.. The state of the art include some examples where other measurements are used in conjunction with the BIS to provide an alert system in the Intensive Care Unit (ICU).

The objective of this case study was to develop models that could predict the value of the BIS using physiological measures.

1.4 Document structure

In this thesis two different types of models were developed: a computational and a hybrid models.

For both models, the state of the art is presented in the next chapter, in order to contextualize the choice of the physiological process underlying each of them. The state of the art chapter is divided in 4 different sections, starting with the definition of physiological systems, some examples, the case studies and a brief conclusion.

Each of the chosen models has its own chapter, starting with the hybrid model (chapter 3). This chapter begins with a description of a drug ingestion model, followed by the adaptation to the three-tank system and an overview of the developed platforms to interface with the model.

Chapter 4 corresponds to the anaesthesia monitoring computer model built using the available datasets. This chapter is divided in a description of the datasets and their analysis, the development of models and a brief discussion.

In the last chapter, the conclusions and future work are presented.

[1] Process is accelerated, instead of taking hours takes minutes

[2] Based on CHUC dataset.

Chapter 2

State of the Art

This chapter starts with a brief discussion about the definition of a physiological model followed by some examples, a review about each of the case studies used in this work and a summary.

In the preparation of this thesis a substantial amount of time was spent during the first semester in the research of different types of physiological systems that could be modelled, such as the liver or the glucose regulatory system.

2.1 Physiological models

Modelling and simulation of physiological systems has long been the subject of interdisciplinary research, especially in recent years with the availability of accurate clinical measurements and powerful computer systems [16].

Seven different generic purposes for physiological models[1] have been identified [17]:

- To determine the structure of a system;
- To compute parameters of interest;
- To integrate information on a system;
- To predict responses to a perturbation;
- To derive mechanistic principles underlying the behaviour of a system;
- To identify differences under different conditions;
- As an educational tool.

As an educational tool, the simulation of physiological systems is a very helpful tool[2]. Coupled with an explanation of the model behind the simulation, it allows the students to observe the behaviour of a system in a low risk environment while providing an insight into the modelled system.

[1] A model can be defined as a simplified representation of a system

[2] To build these simulations, often an iterative process is used in an effort to match the simulations to the real biological systems [2].

Additionally, as simulation often goes together with visualization (the results of changes made by a student can be directly shown on the screen), its usage is appealing to the students [2].

As tool to discover new relations or principles underlying the behaviour of a system, modelling and simulation of physiological systems have helped in the study of their dynamical behaviour and to estimate and optimize parameters that cannot be directly measured.

To build these models, two different types of information can be used: *a-priori* knowledge about the process or experimental data (by measure the inputs and outputs of the system). These models should have two important characteristics [2]:

- Be a simplification of reality (but not too simple that its answers are not true);
- Be simple and easy to use;

A model can be used in three different concepts represented in Figure 2.1.

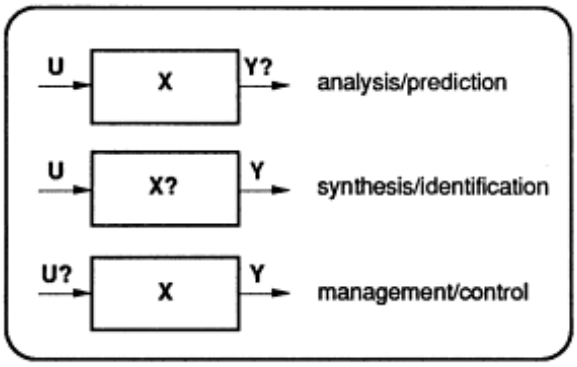

Figure 2.1: Model concepts. (Taken from [2])

From these concepts, the analysis/prediction concept is the one that best fits the systems modelled. In the drug ingestion model, a drug concentration in the body throughout the time is predicted following an ingestion. In the anaesthesia monitoring model, the BIS is predicted using a combination of physiological measures recorded during a surgery.

Models can be classified in several ways: deterministic versus stochastic; linear versus non-linear; kinetic versus dynamic (in [2], the authors identify physiological systems as being normally dynamic) and compartmental versus non-compartmental.

The latter (compartmental) is the most adopted model when physiological systems are modelled. A compartmental system consists of two or more compartments interconnected (when there is exchange of materials by diffusion, chemical reactions, etc.). For example, the ingestion and subsequent metabolism of a drug can be represented by such models [4].

Another interest topic of analysis is the usage of equivalent models using physical systems to describe a physiological system. The variables from each systems have a direct relationship to the physiological mechanisms [18].

For example, the cardiovascular system can be modelled by an equivalent electric circuit (Figure 2.2.(a)) known as the *windkessel model*. In this circuit the voltage represents the blood pressure, the current represents the blood flow, C_p and R_p are the compliance and the resistance of the systemic arterial tree and Z_o the characteristic impedance of the proximal aorta.

Another example is the representation of a skeletal muscle using mechanical elements (Figure 2.2.(b)).

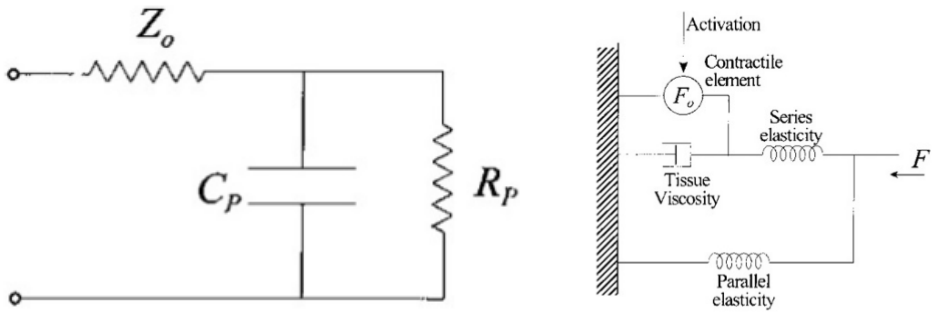

(a) Early analog model of a cardiovascular system. (Taken from [18])

(b) Mechanical analog model of skeletal muscle. (Taken from [18])

Figure 2.2: Analog equivalent models of physiological systems.

One advantage of using physical systems in building equivalent models is the usage of components that have a well-known behaviour to describe quite complicated systems. By using different combinations of these components, a system can be modelled and its mathematical description easily retrieved (by applying the conservation of charge, energy, mass and force laws).

Figure 2.3 is a summary of the equations and forces used in the analogies. A more complete table can be seen in Figure A.1 in appendix A.

Fluid	**Mechanical**	**Electrical**
pressure, P	force, F	voltage, V
volume, V	displacement, x	charge, q
flow, $q=dV/dt$	velocity, $v=dx/dt$	current, $I=dq/dt$
viscous drag, $R=P/q$	viscous reistance, $B=F/v$	resistance, $R=V/I$
compliance, C $q=C \cdot dP/dt$	compliance, $C=x/F$ (stiffness=1/compliance)	capacitance, $C=q/V$ $I=C \cdot dV/dt$
mass, m $P_m=m \cdot dq/dt$	mass, m $F_m=m \cdot dv/dt$	inductance, L $V_L=L \cdot dI/dt$

Figure 2.3: Fluid, mechanical and electrical analogues. (Taken from [3])

In the next section some examples of different physiological models will be reviewed (with the exception of the case studies).

2.2 Examples of physiological models

The work consisted initially in the research of different models of different systems in order to assess which would best fit in this thesis purpose. This search started with a general system search and then a more detailed and compartmentalized system search was performed.

One of the most famous and cited physiological model is the circulatory system model by A.C. Guyton in 1972 [19]. A.C. Guyton and his team developed a model where a whole body circulatory system is represented. This was done by dividing the system into small subsets of organs or major fluid vessels, with the inclusion of their regulatory agents. Using this model, Guyton in 1972 was able to test a variety of physiological hypotheses. In appendix A, Figure A.2 shows this computer model of the cardiovascular system, while in Figure 2.4 a section of this scheme including the kidney and the excretion mechanism can be seen in more detail.

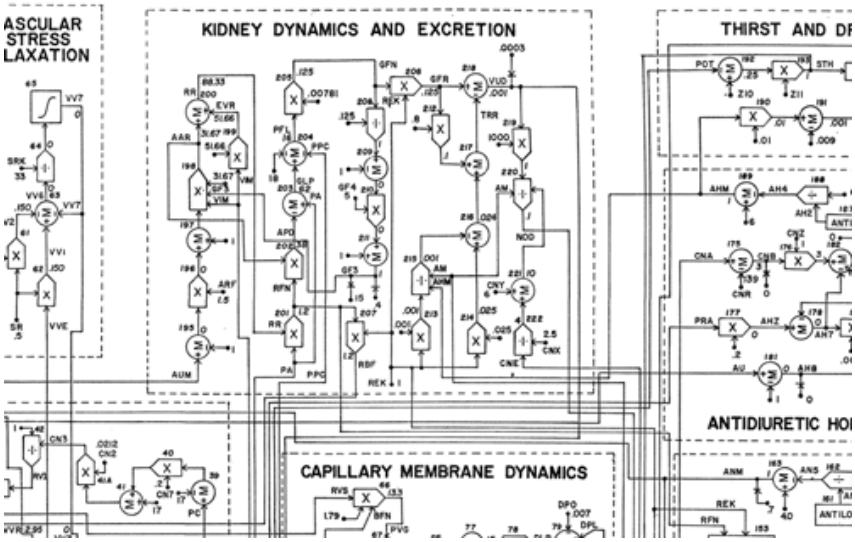

Figure 2.4: Detail section (kidney dynamics and excretion) of the computer model of the cardiovascular system developed by Guyton. (Full model in appendix A, Figure A.2)

Based on the circulatory model and after several improvements, the hummod model [20] provides a platform to understand the complex interactions of integrative human physiology and allows the simulation of different interventions on the human body. Their creators claim it to be "the best, most complete, mathematical model of human physiology ever created", with more than 5000 variables describing the human body physiology and build with the information from a collection of more than 5000 papers.

As mentioned in the previous section, compartmental models are often used to describe and to make predictions on a host of physiological systems. In "WinSAAM: a windows-based compartmental modelling system" [21], the authors describe a platform that can be used to model and simulate linear and non-linear compartmental models, and illustrate some usages in modelling alcohol metabolism, drug metabolism and glucose/insulin kinetics.

After this general overview of systems, a narrower research was performed. One of the systems that aroused the most interest was the liver due to the connection of this research group with the Internal Medicine Unit of the CHUC. About this topic, two different approaches were taken: the review of some metabolic related mathematical models and the review of pure data driven models.

While the first approach returned some interesting results - like the HepatoNet1 [22], an improvement from the metabolic network Recon1, with more than 200 metabolic functions, heavily used in drug research (since it can simulate the effect a certain drug has on the hepatic enzymes and output the changes in some metabolic functions) or a mathematical model of Hepatitis C evolution in a damaged liver [23] (where the evolution of the disease was linked to the density of hepatocytes) - this topic was discarded due to their complexity for the usage in a hospital context.

From the second approach, the black-box models "predicting mortality in patients with cirrhosis of liver with application of neural network technology" [24] (by developing and comparing a neural network capable of predicting one year plus mortality with a logistic regression model and the gold standard, the Child-Pugh's score) and "an intelligent decision-making model combining genetic algorithms and neural networks for hepatic cancer diagnosis" [25] (where a genetic algorithm is used to find the optimal parameters to build a neural network instead of training it) were the most interesting application of data driven models in a hepatic context. It should be noted that both models refer to cirrhosis, since it is the most prevalent liver disorder in the CHUC. This topic was also discarded due to scheduling problems with the CHUC physicians.

Other systems and organs models were researched: Epilepsy [26, 27, 28], due to the connection of one of the supervisors to this topic; Regulatory systems [29, 30, 31, 32, 33, 34, 35, 36, 37], being the most natural systems to be modelled since they can be treated as a control problem; and some other models about the Liver [38, 39, 40, 41, 42, 43, 44].

2.3 Case studies models

After an evaluation process, two different physiological systems, a drug ingestion process and the monitoring of a patient anaesthesia, were selected.

2.3.1 Drug ingestion, progression and excretion models

In [8], the authors define pharmacokinetics as a prediction of the time-dependent concentration of a substance in a living system. There are two different approaches to model this concentration: a classical approach, which utilizes a lumped-compartmental system, and a physiologically based approach, which separates the body into multiple anatomically correct compartments interconnected through the body fluid system.

Although these models are useful, they cannot describe a whole body system composed by different tissues and model the drug affinities for certain organs. By using a classical approach, the solution of the differential equations that describe the system consist on a series of decaying exponentials.

Also in [8], it is mentioned that the first use of a physiological approach in pharmacokinetics appeared in the 1930 [45], when mass balance equations for specific organs were used. Later in 1960 [46], capillary, interstitial and cellular sub-compartments were included in models. Figures A.3 and A.4 in appendix A represent a physiologically based model and the vascular, interstitial and intracellular spaces of an organ.

The ingestion and absorption of a drug can be modelled by a compartmental absorption and transit (CAT) model, where the intestine is divided in a n number of compartments. The usage of this model assumes that there is passive absorption, instantaneous dissolution, linear transfer kinetics for each segment, and minor absorption from the stomach and colon. From the most common drug intake routes (intravenous, subcutaneous, intramuscular and oral ingestion), the absorption model can only be circumvented if an intravenous route is chosen [6].

Other models for drug ingestion and absorption can be seen in [47, 48, 49].

In [6], there is a comprehensive overview of all the factors involved in the transfer of drugs across membranes, delivery systems, distribution, metabolism and excretion. Due to the three-tank system used, some simplifications on the distribution, metabolism and excretion mechanisms had to be made. The distribution and metabolism mechanism are condensed in the excretion mechanism, represented by the drug clearance, or the rate of a drug elimination divided by its concentration.

There are already a number of remote labs using the coupled-tanks process, mainly in water level control problems. In [50], the authors present the design and development of a web-based laboratory experiment used for teaching and do research. In this experiment the user can implement four different controllers (manual, PID, state-space or fuzzy knowledge) for a two coupled tank experiment.

A similar lab is presented in [51], where the authors use a three-tank process similar to the one used in this thesis. In this remote lab, the user can 'control' the valve opening between and out of the tanks[3] and control the pumps. It also provides a simulated view of the process, a live feed or an augmented view (overlay of the simulated view on top of the live view).

In the next chapter, the equations, simplifications and parallel made between a drug ingestion, progression and excretion model and the three-tank process used will be explained.

[3]The interface allows for the specification of the valve opening, but when in operation the opening is manually controlled.

2.3.2 Anaesthesia monitoring

Monitoring the state of a patient subjected to general anaesthesia is a difficult and a highly demanding task for the anaesthesiologist. General anaesthesia of a patient is maintained by a combination of hypnotic agents, inhalational agents, opioids, muscle relaxants, sedatives, and cardiovascular drugs, along with ventilatory and thermoregulatory support [52].

In [52], they identify heart rate and blood pressure rapid changes, perspiration, tearing, changes in pupil size, the return of muscle tone, movement and changes in EEG measures of brain activity as indicators of inadequate general anaesthesia. Four EEG patterns defining the phases of the maintenance period are also shown, as well as the description of the changes expected when emerging from anaesthesia state and the mechanism of unconsciousness induced by general anaesthesia (details of the changes in the nervous system).

Similar to the liver, a research into intelligent models was done: In [53] a rule based model that generates two types of alarm depending on the seriousness and quickness of response, aiding the anaesthesiologist in noticing changes in the patient earlier was described. In [9] a clinical decision support and closed-loop control for cardiopulmonary management and intensive care unit sedation using expert systems was presented. These systems combine the current formula to obtain the dose of a sedative agent in the ICU, the Motor Activity Assessment Score, with other variables, and using a Bayesian network to predict the correct sedative agent. A graph representing this network can be seen in appendix A Figure A.5.

In the last decade, a new system is being used to aid in assessing the patient anaesthesia. This system returns an index named the bi-spectral index, or BIS, which is based on the inter frequency phase relationships in the electroencephalogram (EEG) and incorporates features that correlate with the effects of hypnotic drug (derived from a large patient database) [54]. It was reported to be efficient on predicting responses to noxious stimulation during propofol anaesthesia [55]. This monitoring type is one the techniques that uses objective methods.

Other approaches exist that consider temperature, ventilation, hearth rate and other variables. Those approaches are considered subjective monitoring, because they depend on the anaesthetist evaluation [56]. In [57] an overview of both objective and subjective methods is provided.

However, this index is not being used in a widespread way as an absolute indicator of patient awareness. The lack of studies that prove the effectiveness of the BIS index limits its wide acceptance[58], while in [59] their findings do not support routine BIS monitoring as part of standard practice. Nevertheless, the BIS was reported as a tool to decrease some post operation delirium and cognitive decline in elderly people [60] and to help reducing the requirement of propofol for sedation during regional anaesthesia [61]. In [62], the authors conclude that "the relation between BIS and sedation depth may not be independent of anesthetic agent. Quality of recovery was similar between drugs, but excitement occurred frequently with sevoflurane" and that the "BIS was a better predictor of propofol sedation than sevoflurane or midazolam". In the available datasets, the drugs used were mainly sevoflurane and propofol.

Another topic of interest in the subject of anaesthesia monitoring is the relation between the BIS and other physiological variables. In [63], the authors found that between four electrophysiological variables (the BIS, 95% spectral edge frequency, median frequency and the auditory evoked potential index (AEP)), the BIS was the variable that best correlated with the concentration of propofol, while the AEP index appeared to distinguish the awake from asleep state. In [64], the authors compare their scale to monitor or quantify sedation of patient in the ICU - the Sedation-Agitation Scale (SAS) - against the BIS and another scale, the Visual Analog Scale (VAS). Their conclusion shows that the SAS agreed with the BIS and the VAS for long term monitoring of a patient sedation level in the ICU.

2.4 Summary

In this thesis two different process were modelled: a drug ingestion, propagation and excretion process and an anaesthesia monitoring process. These processes were chosen due to either the specific laboratory equipment available (hybrid model) or the datasets available (anaesthesia models).

In the first model, a classic approach to model the pharmacokinetics of drugs was used. After the development of this, an equivalent model was developed to simulate the process using a three-tank system. In the end, this equivalent model was integrated into a remote lab environment to be used as a research and educational tool. Due to the limitations of the laboratory equipment, a classical approach was used, the intestine was represented by one compartment and the ingestion was modelled by the flow of a water pump.

In the second model, a relation between one index used to monitor the state of anaesthesia of a patient (the BIS) and other recorded variables was found, in an effort to find an index that could be used when there missing values.

Chapter 3

Modelling and simulation of a physiological process using a remote lab

In this chapter the steps taken to develop and integrate a physiological model for a drug ingestion, propagation and excretion into a remote lab are presented.

3.1 Drug ingestion, propagation and excretion model

When reviewing the literature, it was found that a compartmental model for pharmacokinetics was the best fit for this process. The simplest model is using a two-compartment system, modelling the gastrointestinal (GI) tract, bloodstream and their interactions. Figure 3.1 is an illustration of this approach.

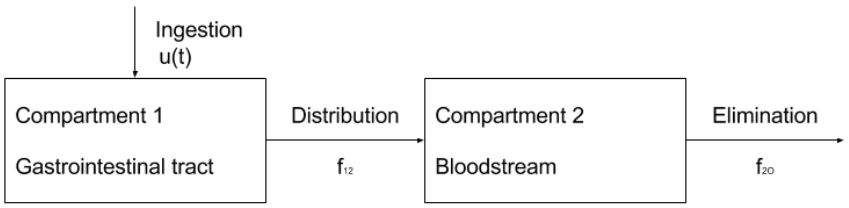

Figure 3.1: Two-compartment drug ingestion and metabolism model. (Adapted from [4])

After oral ingestion, the drug enters the GI tract, where it is absorbed to the bloodstream. Afterwards, it is distributed throughout the body to be metabolize and finally eliminated.

For the first compartment, the variation of the mass of drug in this compartment can be modelled by equation 3.1.

$$\frac{dq_1(t)}{dt} = u(t) - f_{12}q_1(t) \tag{3.1}$$

In equation 3.1, $q_1(t)$ represents the mass of the drug in compartment 1 at a certain t time, $u(t)$ the ingestion rate and f_{12} a proportional constant to the mass (or concentration) of a drug in the compartment (in the simplest case of first-order kinetics). This equation is a mass balance equation.

The same can be determined for the second compartment (equation 3.2).

$$\frac{dq_2(t)}{dt} = f_{12}q_1(t) - f_{2O}q_2(t) \tag{3.2}$$

In this equation, the first term of the difference represents the inflow rate to the compartment (flowing from the first to the second compartment) and the second term the outflow rate from the compartment. Applying the assumption of first-order kinetics, this second term is assumed to be proportional to $q_2(t)$ (the mass of the drug in compartment 2), with f_{2O} the new constant of proportionality.

Another compartment can be added to this model, the bladder, following the same approach and first-order kinetics. Figure 3.2 is an illustration of this approach.

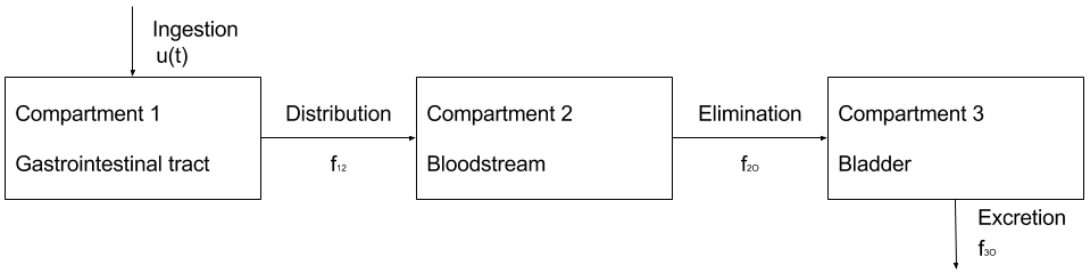

Figure 3.2: Three-compartment drug ingestion, metabolism and excretion model.

The third tank model, like the human bladder, has 3 different conditions: it can be filling up, it can be holding the current amount of liquid or it can be releasing fluid.

$$\frac{dq_3(t)}{dt} = f_{2O}q_2(t) \tag{3.3}$$

In the filling up condition, equation 3.3, the changes in the mass of drug in the compartment ($q_3(t)$) are due to the elimination of the drug from the bloodstream (compartment 2).

When there is no elimination in the second compartment, equation 3.3 yields to 0, the second condition. In this condition, the mass of drug in the compartment is kept unchanged.

If this mass crosses the maximum amount of allowed by the system, then the bladder is emptied. Equation 3.4 represents this new condition.

$$\frac{dq_3(t)}{dt} = -f_{3O}q_3(t) \tag{3.4}$$

3.1.1 Example - Paracetamol intake

Paracetamol (also called acetaminophen) is a widely used analgesic and antipyretic agent.

Some of the parameters that describe a drug and the effects it has on the body are[1]: bioavailability (fraction of a dose of drug that reaches the systemic circulation in an unchanged form [65]), absorption rate constant, volume of distribution (proportionality factor between the total amount of drug present in the entire body and the concentration on the plasma [66]), clearance (measure of the ability of the body/organ to eliminate a drug from the blood circulation [66]), extraction rate constant and the time to peak concentration in plasma.

Some of these parameters can be calculated, for example the rate of excretion and the rate of absorption. In [67], equations 3.5 and 3.6 are used to calculate this rates.

$$C_l = k_e \; . \; V_d \;\; <=> \;\; k_e = \frac{C_l}{V_d} \tag{3.5}$$

$$t_{max} = \frac{ln(k_a) - ln(k_e)}{k_a - k_e} \tag{3.6}$$

In equation 3.5, C_l is the total body clearance and V_d is the volume of distribution. In equation 3.6, k_a is the rate of absorption and t_{max} is the time to peak concentration in plasma. In both equations k_e is the rate of extraction/elimination.

For paracetamol, the value for clearance, volume of distribution and time to peak concentration are described in [68]. Table 3.1 contains these values plus the mass ingested and the calculated rates using the equations above.

Table 3.1: Variables used to simulate a paracetamol ingestion, in fasting and using a oral solution.

Variable	Value
Bioavailability	90 %
Clearance	22.8 (l/h)
Volume of distribution	65 (l)
Time to peak	15 (min)
Body weight	70 (kg)
Ingested drug	840 (mg)
Rate absorption	15.517 (h^{-1})
Rate elimination	0.35 (h^{-1})

To simulate an ingestion, equations 3.1 and 3.2 were used. In equation 3.1, $u(t)$ is zero considering that all of the paracetamol is available in the intestines at $t = 0$. A situation where $u(t)$ would not be zero is when a slow release tablet is considered, where the paracetamol is slowly made available in order to maintain a certain concentration in the blood.

[1]When it is considered an oral ingestion

In equation 3.2, $f_{12}q_1(t)$ is multiplied by the bioavailability and then divided by the volume of distribution to reflect the concentration of the drug in the blood.

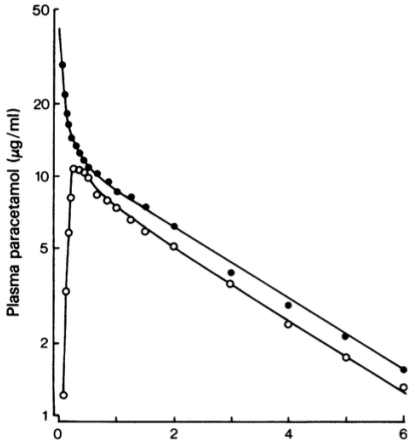

(a) Mean plasma concentrations of paracetamol. White circles is data from a 12 mg/kg oral doses. (Taken from [68])

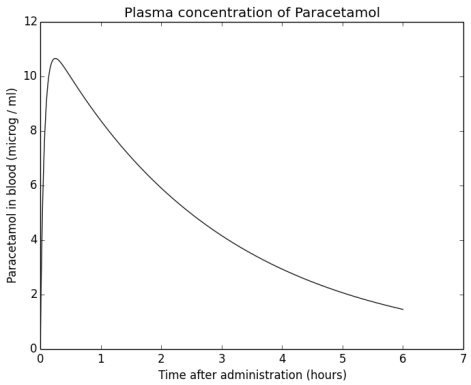

(b) Simulated oral ingestion of a 12 mg/kg oral dose.

Figure 3.3: Comparison between real patient data and simulation.

Figure 3.3.(a) and 3.3.(b) are two different oral ingestion of 12 mg/kg doses of paracetamol, one from real data and taken from [68] while the other is a simulation using the values from Table 3.1.

In both, the peak concentration value and the time to this peak are very similar.

In [68] it is also mentioned that absorption from tablets is slower, taking approximately 1 hour to reach the peak concentration.

Recalculating the absorption rate for the tablets, the new value for k_a is 2.19 h^{-1}. The result of the simulation for the oral intake of tablets of paracetamol is displayed in Figure 3.4 in blue.

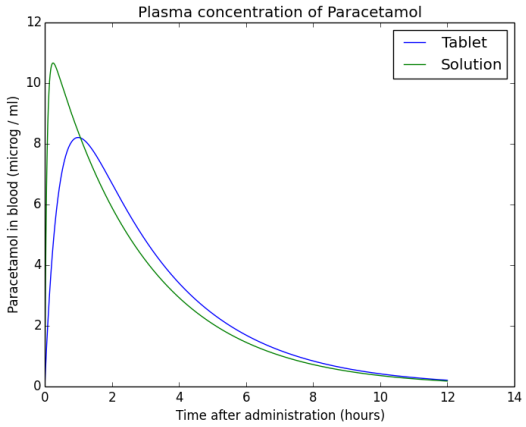

Figure 3.4: Overlay between a simulated intake of paracetamol using two different processes: solution and a tablet.

Due to a slower absorption rate, the time to the peak concentration is higher and the value for this peak is lower.

In summary, in order to use a two-compartment first-order drug pharmacokinetic model for any drug, the values of Table 3.1 have to be known.

3.1.2 Equivalent model

An obvious equivalent model for the ingestion, progression and excretion model is the amount of fluid in leaky tanks [4], as pictured in Figure 3.5 for the two-compartment ingestion and metabolism model.

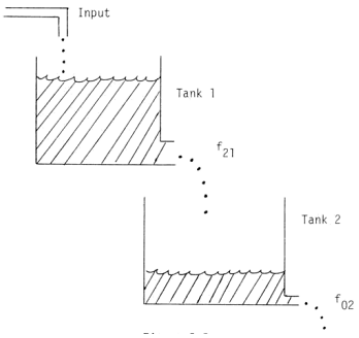

Figure 3.5: Two-tank equivalent model for the process represented in Figure 3.1. (Taken from [4])

In this equivalent model, the mass of a drug is represented by the change in water level from a reference level.

For this thesis a three-tank system was used as an equivalent model. Figure 3.6 is a picture of the system used, the DTS200 three-tank system manufactured by Amira GmbH (for more technical information [51] or [5]).

Figure 3.6: Three-tank system by Amira. (Figure taken from [5])

The system used is not the ideal equivalent model. A cascade system (like the one represented in Figure 3.5) is a better model, since all the tanks are mass uncoupled. This mass uncoupling does not occur in the system used, imposing some level restrictions to the coupled tanks. For example, the level of the centre tank cannot be higher than the level of the left tank, since flow from the centre to the left tank is not assumed.

To best represent the three-compartment model, the three-tank system was divided into two sections separating the GI tract and the bloodstream from the bladder. A scheme of this division can be seen in Figure 3.7.

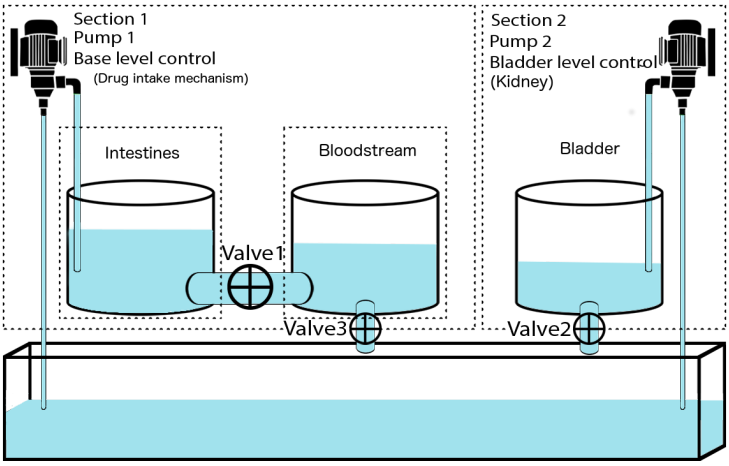

Figure 3.7: Scheme for the division of the three-tank system.

By using such division, the level constraint imposed by the right tank (because of the mass coupling) on the rest is eliminated and the control of the right tank is easier.

$h_l(t)$ and h_{l0} are the left tank current and reference water level, $h_c(t)$ and h_{c0} are the centre tank current and reference water level and $h_r(t)$ and h_{r0} are the right tank current and reference water level.

c_{lc} is the flow coefficient between the left and centre tank and c_{co} and c_{ro} are the outflow flow coefficients of the centre and right tanks, respectively.

$f_{p1}(t)$ is the flow pumped by the pump$_1$.

In Table 3.2, a relation between the equivalent and physiological model variable is presented

Table 3.2: Relation between the physiological and the equivalent model variables.

Physiological model		Equivalent model	
Variable	Description	Variable	Description
$q_1(t)$	Mass quantity first compartment	$h_l(t)$ - h_{l0}	Level difference left tank
$q_2(t)$	Mass quantity second compartment	$h_c(t)$ - h_{c0}	Level difference centre tank
$q_3(t)$	Mass quantity third compartment	$h_r(t)$ - h_{r0}	Level difference right tank
f_{12}	Flow from the first to the second compartment	c_{lc}	Flow coefficient from the left to the centre tank
f_{O2}	Flow from the second to third compartment	c_{co}	Flow coefficient for the centre tank outflow
f_{O3}	Outflow from the third compartment	c_{ro}	Flow coefficient for the right tank outflow
$u(t)$	Inflow for the first compartment	$f_{p1}(t)$	Inflow for the left tank

3.2 Three-tank system model

3.2.1 Right tank (Bladder) equations

The right tank of the three-tank system (Figure 3.7) is used as a virtual bladder, absorbing the perturbation caused by the drug intake. The water level is controlled by the pump_2, which is acting as a virtual kidney.

When the water level reaches a certain threshold, the bladder stops absorbing the perturbations and empties. Figure 3.8 represents the bladder tank (section two) of Figure 3.7.

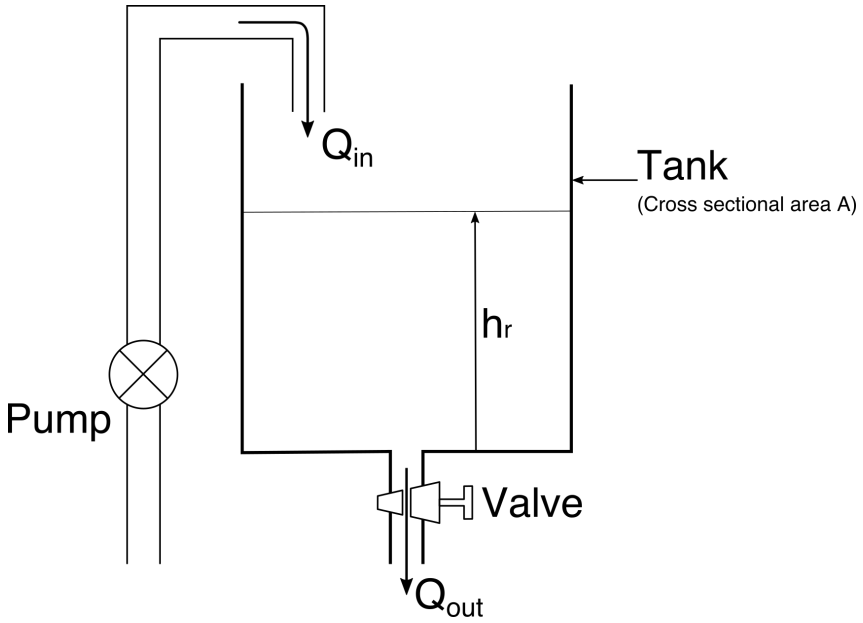

Figure 3.8: Right tank representation.

Considering that the top of the water column and the discharge valve are at the same pressure (in this case atmospheric pressure), the flow rate at the valve is [69, 70]:

$$Q_{out}(t) = ac\sqrt{2gh(t)} \tag{3.7}$$

With a being the cross section area of the discharge pipe, c the flow coefficient for the discharge pipe, g the gravitational acceleration and h the water level of the tank at the current time t.

Using the mass conservation equation, the variation of level with time can be obtained using 3.8.

$$\triangle V(t) = dh(t)A$$

$$\triangle V(t) = (Q_{in}(t) - Q_{out}(t)) \times dt \tag{3.8}$$

$$\frac{dh(t)}{dt} = \frac{Q_{in}(t) - Q_{out}(t)}{A}$$

In equation 3.8, A refers to the cross section area of each tank.

Replacing equation 3.7 in 3.8:

$$\frac{dh(t)}{dt} = \frac{Q_{in}(t) - ac\sqrt{2gh(t)}}{A} \tag{3.9}$$

Equation 3.9 represents the variation in level for a single tank.

For the the right tank used in this work, then 3.9 yields 3.10.

$$\frac{dh_r(t)}{dt} = \frac{f_{p2}(t) - ac_{ro}\sqrt{2gh_r(t)}}{A} \tag{3.10}$$

In equation 3.10, $f_{p2}(t)$ is the flow being pumped by the pump_2 into the right tank, and is controlled depending on the current bladder condition.

If the bladder is filling, then the pump_2 flow will be proportional to the outflow of the centre tank. On the other hand, if the bladder is emptying then the flow will be zero.

If the bladder is maintaining the level of water inside, then the flow of the pump will be equal to the flow of water exiting at the current height.

3.2.2 Left and centre tanks (Intestines and bloodstream) equations

The left and centre tanks of the three-tank system act as the intestines and bloodstream, respectively, while pump_1 serves as an intake mechanism, increasing the water level of the left tank. This perturbation is then passed on to the centre tank and later excreted by the right pump into the right tank. Figure 3.9 represent this two-tank section (section one in Figure 3.7).

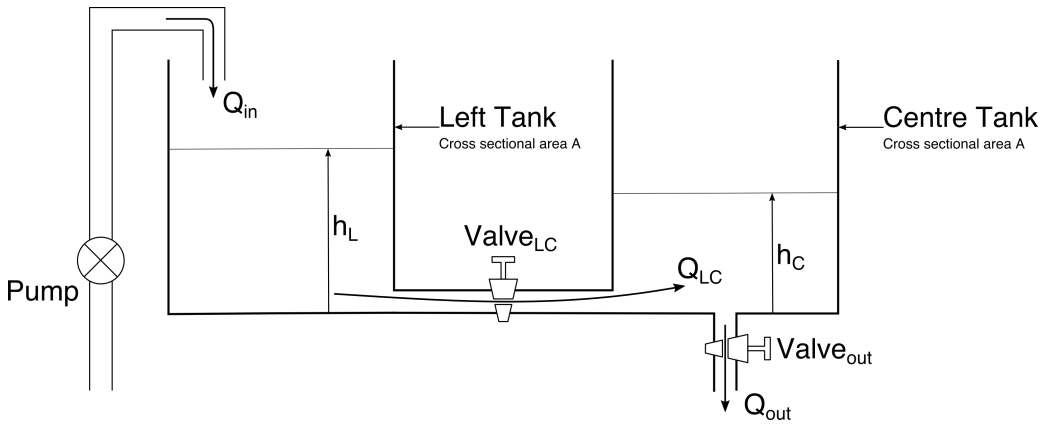

Figure 3.9: Coupled tanks fluid level system, with one input and one output.

By applying the mass conservation equation, the variation of level with time for each tank can be obtained. The left tank is represented by equation 3.11 and the centre tank is represented by equation 3.12.

$$\frac{dh_l(t)}{dt} = \frac{Q_{in}(t) - Q_{LC}(t)}{A} \tag{3.11}$$

$$\frac{dh_c(t)}{dt} = \frac{Q_{LC}(t) - Q_{out}(t)}{A} \tag{3.12}$$

Assuming each flow obeys the Bernoulli equation[2]:

$$Q_{LC}(t) = ac_{lc}\sqrt{2g(h_l(t) - h_c(t))} \tag{3.13}$$

$$Q_{out}(t) = ac_{co}\sqrt{2gh_c(t)} \tag{3.14}$$

Replacing equations 3.13 and 3.14 in equations (3.11) and (3.12), the final equations representing the variation of each tank water level can be obtained:

$$\frac{dh_l(t)}{dt} = \frac{Q_{in}(t) - ac_{lc}\sqrt{2g(h_l(t) - h_c(t))}}{A} \tag{3.15}$$

$$\frac{dh_c(t)}{dt} = \frac{ac_{lc}\sqrt{2g(h_l(t) - h_c(t))} - ac_{co}\sqrt{2gh_c(t)}}{A} \tag{3.16}$$

3.2.3 Model considerations

To tune the parameters of the three-tank system to model and simulate a drug ingestion, progression and excretion, an analysis of a drug mass evolution in the human body with time was done.

In Figure 3.10 a generic drug concentration evolution for a single dose oral administration is represented, with a very similar curve as the curves in Figure 3.4

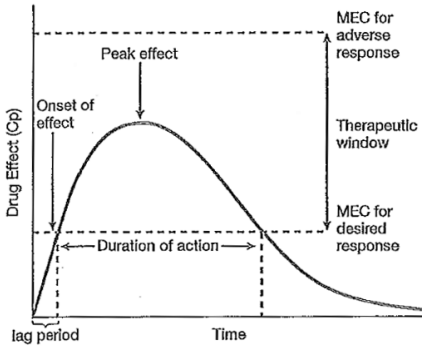

Figure 3.10: Temporal characteristic of a drug effect for a single dose oral administration. Cp represents the plasma drug concentration. (Taken from [6])

[2]In equation 3.13 it is assumed that the flow of water only occurs from the left tank to the centre tank.

There are two main phases in this figure: before the peak and after the peak. Before the peak, the drug concentration increases as the drug continues to be absorbed and distributed. When the peak is reached, the elimination period starts[3].

The controller for the right tank (bladder) only starts to accumulate water when this peak is reached, to simulate this elimination period.

In the simulation of the absorption of paracetamol, it is considered that all the paracetamol is available for absorption in the beginning of the simulation. This phenomena is not possible to replicate since there are not any computer controlled valve, which would allowed to accumulate all the water needed to represent the mass of the drug.

Also, since the valve in between both tanks allows flow in both directions, the tank representing the intestine cannot be fully depleted. In fact, the level of the left tank has to be always higher than the level of the centre tank. Due to this constraint, the mass of the drug is represented by the difference in height to a reference level.

Finally, since the escape valve in the left tank is kept closed, it is assumed that all the drug ingested is absorbed.

For a tablet (1 hour to peak time) of orally ingested paracetamol, the rates of absorption and elimination are 2.19 and 0.35 h^{-1} respectively. The only constant that can be changed in the equivalent equations is the flow coefficient.

In order to model the absorption rate, the valve between the left and centre tanks was opened 75%. This percentage allows for a easier replication of the experiment if for some reason the position of the valves is changed. From experimentation (view appendix B) the value for the flow coefficient when the valve is open approximately at 75% is 0.4180.

When comparing with the value for the absorption rate, it is approximately 5.2 times less. Assuming the 5.2 times relation, the flow coefficient for the outflow valve in the centre tank should be approximately 0.067 (12%), a value very difficult to replicate due to technical reasons.

With these values for the flow coefficients, with no height restriction and using a flow value of 8.08 cm^3/s (0.5 V control signal) to maintain the steady state base level, it take a 3510 s ingestion at a 98.9 cm^3/s (5 V) flow to achieve the peak height concentration in the centre tank 1 hour after the start of the ingestion[4]. The level difference at this point is around 7.6 m (Figure 3.11).

[3]The elimination process occurs in parallel with absorption. When the peak is reached, the elimination process surpasses the absorption process

[4] For a tablet of 12 mg/kg of Paracetamol it takes approximately 1 h to reach the peak concentration

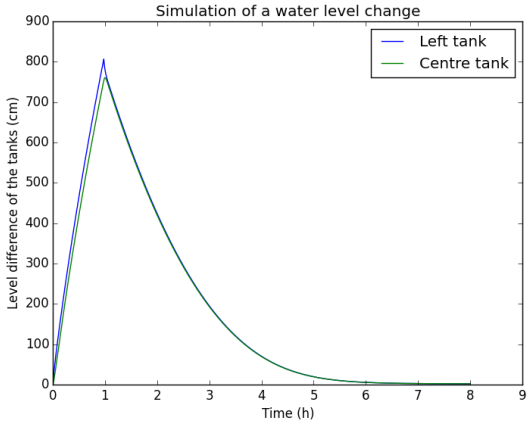

Figure 3.11: Simulation using the first iteration of an equivalent model.

Since there are height restrictions to the system (less than 60 cm) and the position of the second valve had to be a value easily replicated, new relations were found.

For the valve position, 25% was the value chosen. This value is easily replicated and the flow coefficient is 0.1814 (the determination of the flow coefficients is presented in appendix B), 2.7 times higher than the older outflow flow coefficient value. Since the value of the outflow valve is higher, the intake flow was also raised from 8.08 to 24.21 cm^3/s.

Using this flow coefficient, the peak of the level difference still occurs approximately 1 hour after the ingestion, but the water level is still too high at 3.56 m (2.13 times smaller. It is not 2.7 times smaller due to the fact it depends of both flow coefficients). Figure 3.12 represents this simulation.

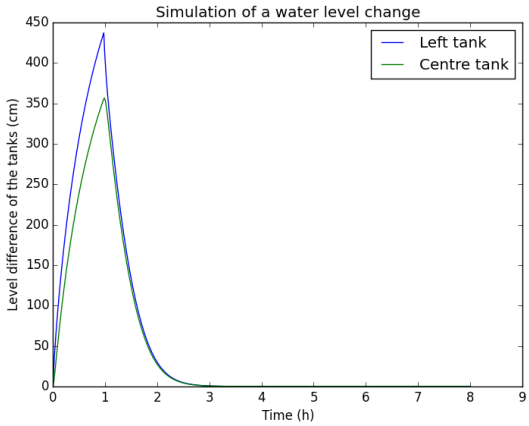

Figure 3.12: Simulation using the second iteration of an equivalent model.

The next step was to decrease this peak and the time to reach it. First, the ingestion time was cut by a factor of 100, making it 35 s and, as a precaution, the ingestion flow was lower from 98 to 78.64 cm^3/s (5 to 4 V).

By cutting the ingestion duration, the time to peak was reduced from 3600 to 172 s and the peak of the level difference was reduced from 7.6 to 0.05 m, a value 152 times lower.

In conclusion, by using an outflow flow coefficient 2.7 times higher and an ingestion time 100.29 times lower to simulate an oral ingestion of a 12 mg/kg oral tablet the final result is a concentration 152 times lower, a time to peak 20.93 faster and an overall time in body 6 times lower (approximately 6 h in Figure 3.11 and 1 h in Figure 3.13).

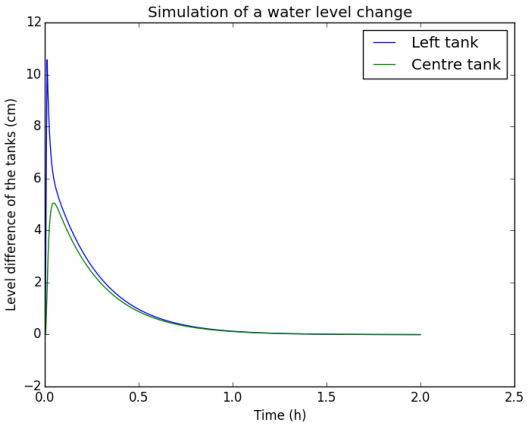

Figure 3.13: Simulation using the final equivalent model.

In order to verify this relations, they were applied to a simulation of an adapted ingestion. Figure 3.14 is a comparison between the expected and a rescale.

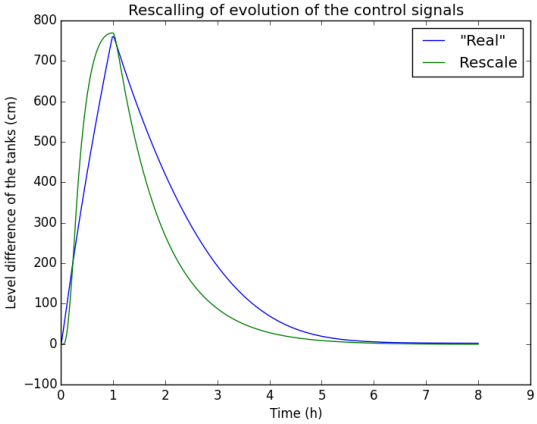

Figure 3.14: Comparison between a "real" ingestion and a rescale of an adaptation.

The plots are very similar, but, since there are different approximations and the effect of the left tank is different in both experiments, the curves do not match perfectly. The rescale curve has decay rate higher than the expected (the rate of the "real" curve), reaching lower drug concentrations (water level differences) faster.

3.2.4 Controllers

In this section an overview of the controllers used in this work is provided. For the first section (the left and centre tanks), $pump_1$ control signal is always 1.3 V to maintain the desired reference level, except when there is an ingestion. The right tank control scheme is explained below.

Right tank (bladder) controller

This is the general control routine for the right tank. There are three main control decision points, two control processes (Release Water, described in the flowchart, and Height Control, described latter and represented by Figure 3.17), and two major routines: filling up/maintaining the level of the virtual bladder and its discharge.

The outcome of each control process return an updated target height, which will be used to drive the pump controller.

These control routines are represented by the flowchart in Figure 3.15.

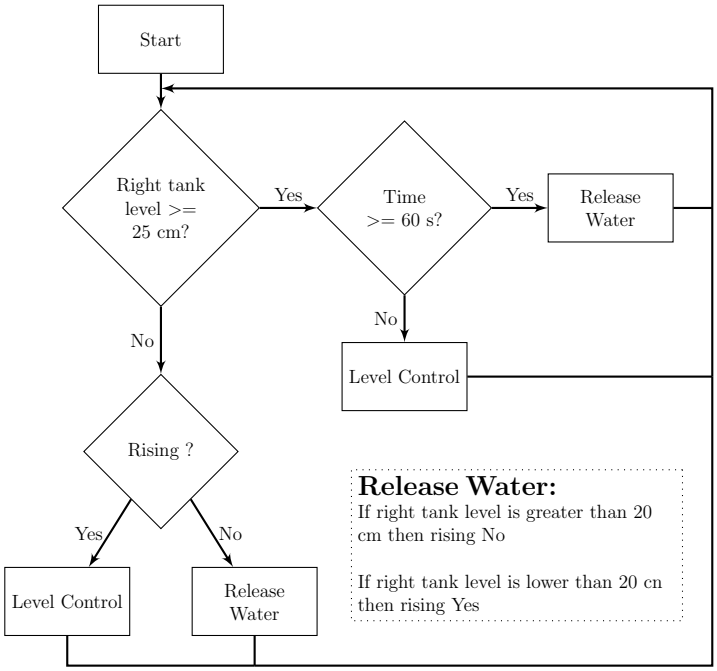

Figure 3.15: Right tank level controller flowchart.

During the filling up phase (due to perturbations in the centre tank, the bloodstream) or in maintaining the current level, the control is handled by the Level Control process (Figure 3.17). If the level of the tank surpasses 25 cm, the Level Control process remains in control of the tank for a period of 60 s (simulating the time a person would need in order to reach a bathroom). After this period, the control of the bladder passes to the Release Water process until a level of 20 cm is reached, returning then the control back to the Height Control process.

By using this simple controller, the two major functions of a bladder can be modelled and afterwards simulated: the accumulation of liquid and its excretion. A level of 20 cm was set as the lower limit due to the instability caused by the valve when the water level is low. The threshold was set as 25 cm as an arbitrary level so a discharge could be seen in the simulation window.

In the human body, when the amount of liquid inside the bladder reaches a volume close to 350 /400 ml, a person becomes uncomfortably aware. This sensation is given by stretch receptors in the bladder wall. From 400 to 600 [7] or 700 ml [71], the pressure and awareness of a full bladder increase steeply. At 600/700 ml, there is the sensation of pain and often there is a loss of voluntary control [71]. Figure 3.16 represents the relation between the pressure and volume inside the bladder for a normal situation. There is a plateau from 100 ml up to 350 ml due to the adaptability of the bladder muscles [7].

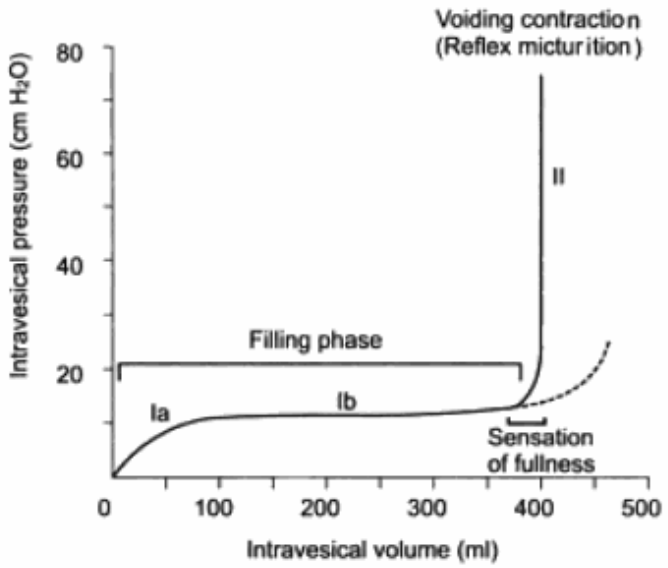

Figure 3.16: Relation between the pressure inside the bladder and the volume accumulated. (taken from [7])

This process is controlled by the brain, corresponding to the right tank controller, and mediated by afferent[5] pelvic nerves, corresponding to the discharge threshold.

Level control process

The main function of this process is to check if there was a change in the water level in the centre tank and if so an action has to be taken. In this process there are two main decision points and two possible outcomes (increase the water level of the right tank or maintaining it).

This control routine is represented by the flowchart in Figure 3.17.

[5]Long nerves connection from a sensory receptor/organ towards the central nervous system. From the Latin *afferentem*, carrying info.

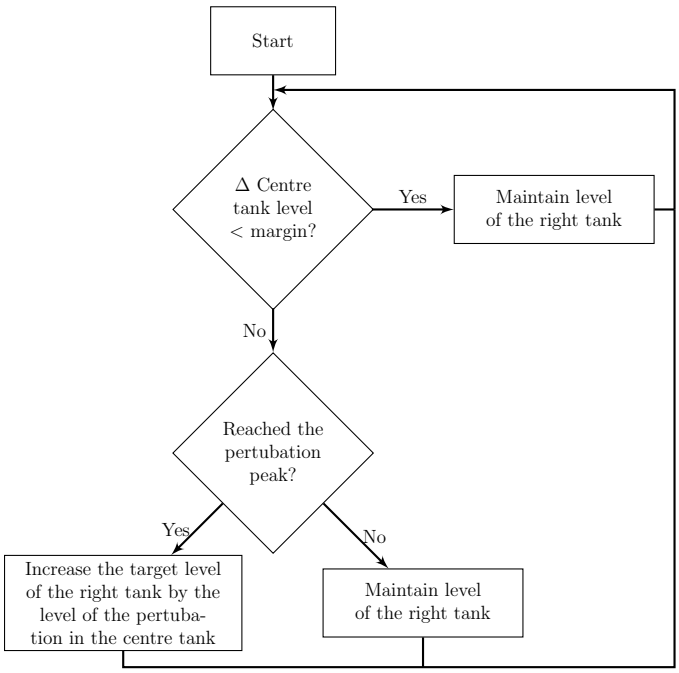

Figure 3.17: Right tank process flowchart included in the level control flowchart (Figure 3.15.).

If the level of the centre tank does not surpasses a threshold plus a margin (due to noisy nature of the read signal), pump_2 has a flow that maintains the current water level in the right tank (the right tank target level is not changed). If the margin is surpassed, but the centre tank is still filling (the peak is not found), the level is also not changed.

It is only when the peak of the perturbation in the centre tank is reached that the target level of the right tank is changed to reflect the perturbation. This controller ensures that only the variation between the resting level of the centre tank to the peak of the perturbation is absorbed by the right tank.

Right pump controller

The pump_2 voltage is proportional to a certain level established for the right tank. This target level is set either by the Release Water process or the Level Control process. A simple proportional controller can be designed to fulfil this purpose.

A proportional controller (PC) can be defined as a simple linear control algorithm characterized by a constant relationship between the controller input and output [72]. Equation 3.17 represents the PC implemented.

$$u_2(n+1) = K_c \times (h_r 0 - h_r(n)) \tag{3.17}$$

In equation 3.17, K_c represents the adjustable parameter of the proportional mode, h_{r0} and $h_r(n)$ the target and current height for the right tank and $u_2(n+1)$ the new control voltage for pump_2. Changes in the centre tank will change the target level of the right tank. Each time a new target level is set, it will cause the controller to adjust the control signal for the pump in order to bring the current level to the established by the target level.

The adjustable parameter K_c was found by trial and error and one of the best values found was 49.349.

To test the performance of the controller, two simulations were done: one when there was no discharge and another when there was a discharge. In Figure 3.18 the plot for the change in water level and change in control signals are shown.

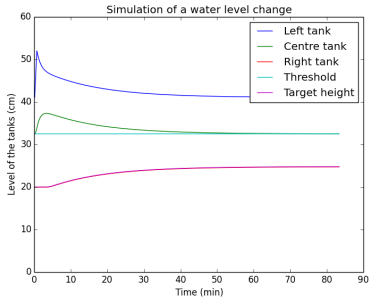

(a) Simulation of change in the tanks water level. Discharge threshold of 25 cm.

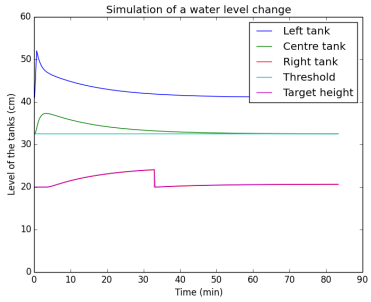

(b) Simulation of change in the tanks water level. Discharge threshold of 24 cm.

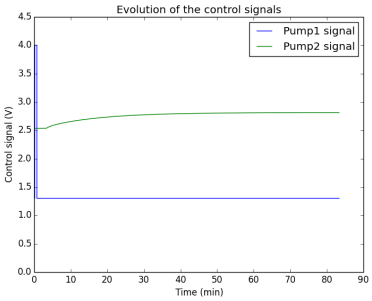

(c) Simulation of change in the pumps control signal. Discharge threshold of 25 cm.

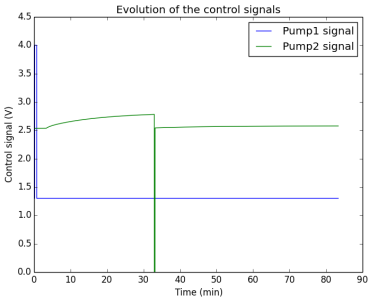

(d) Simulation of change in the pumps control signal. Discharge threshold of 24 cm.

Figure 3.18: Comparison between two thresholds

As it can be seen in Figure 3.18.(b), when the right tank surpassed the level of 24 cm, there was a fall in the tank level. In Figure 3.18.(d), the green control signal is increasing, until the right tank surpasses the threshold and the control signal goes to 0 V[6]. When the right tank level is 20 cm, then the pump increases the control signal again, resuming the function of accumulating water.

3.3 Simulation platforms

3.3.1 Computational only

A web-based computational only platform (simulating an interaction with the remote laboratory) was adopted in order to cover network-based failures (for example an offline server or if the power is down) of the online remote laboratory, allowing the user to perform a drug ingestion simulation. Figure 3.19 provides an overview of the user interface.

[6]Lower saturation value.

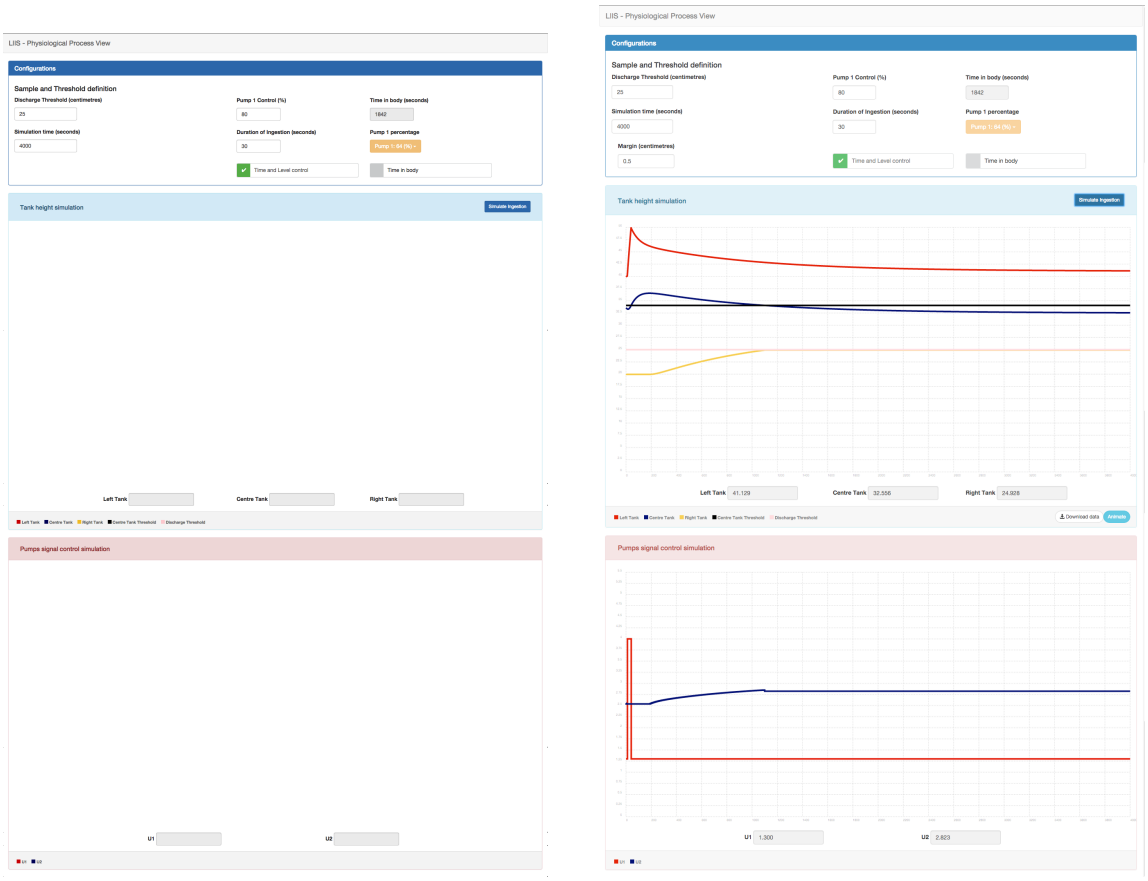

(a) Screenshot before simulating an ingestion.

(b) Screenshot after simulating an ingestion.

Figure 3.19: Screenshots of the online simulation platform.

There is also an option to save the simulation data[7] and an animation, mimicking the evolution of the system when it is used online. (Figure 3.20).

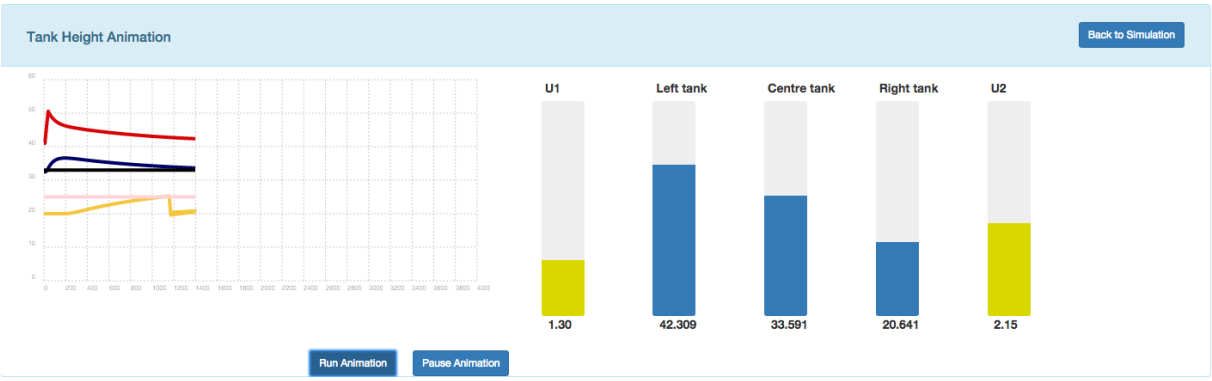

Figure 3.20: Animation option for a simulation of a drug ingestion.

[7]Only available when using the Chrome browser.

There are multiple input options for configuring the simulation as it can be seen on Figure 3.21.

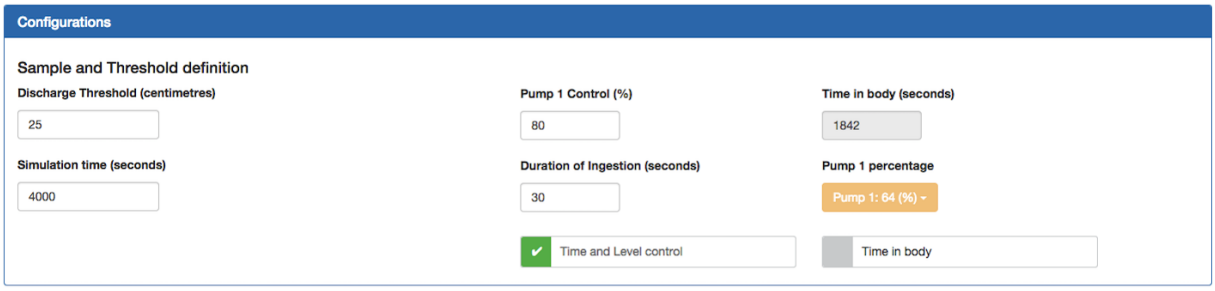

Figure 3.21: Configuration panel.

On the left side of the configuration panel (Figure 3.21), the user can insert the discharge threshold (limited between 20 and 60 cm) and the duration of the simulation.

In the centre of the configuration panel, if the check box is ticked, the option of manually inputting the percentage of flow for pump_1 and the duration of its effect is unlocked. The percentage must be between 26 and 100%, while the duration of ingestion must be higher than 30 s. If the ingestion time is too high, the left tank will saturate and pump_1 will toggle between the chosen percentage and the base percentage.

When choosing a percentage for pump_1 or the duration of ingestion, both values are compared against a limit. If this limit is surpassed, a warning pop-up window appears with the option to auto adjust the settings to avoid saturation (Figure C.1.(a) in appendix C). Figure C.1.(b) in appendix C shows an example of a saturated signal and the warning pop-up window that appears to the user.

To find the limit aforementioned, a series of simulations were performed. For each control voltage in a range between 2 to 5 V, small increments in 0.1 V were used. For each new voltage, 870 simulations were run using ingestion times starting at 30 and ending at 900 s. The result of these runs can be seen in Figure 3.22.

The red line in Figure 3.22.A and Figure 3.22.B were found using the second derivative of each blue line (the intake time vs. the time in the bloodstream) in Figure 3.22.A, since there are two clear visible regions.

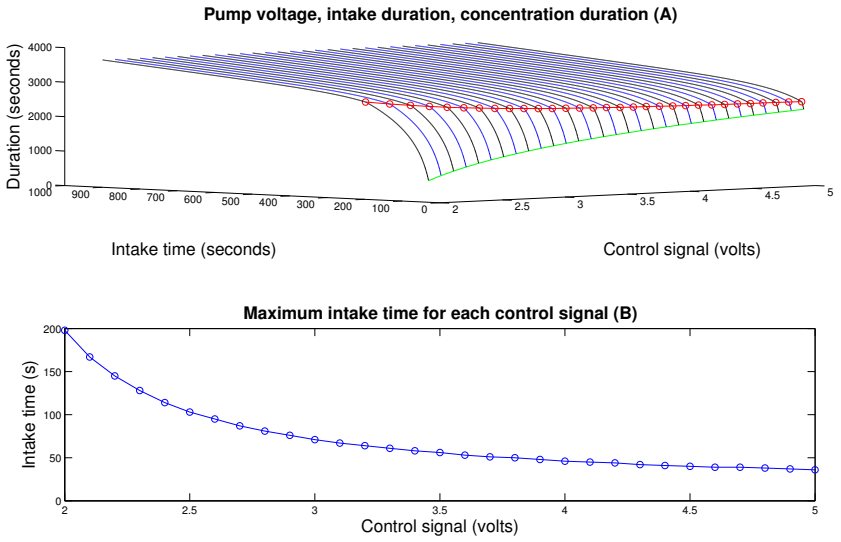

Figure 3.22: Result of 26100 simulation (870 intervals time 30 control signals) in order to find the saturation limit of the left tank for a series of different pump_1 settings.

The points were fitted using a seven order polynomial function, as represented in Figure 3.23 and described in Table C.1, appendix C.

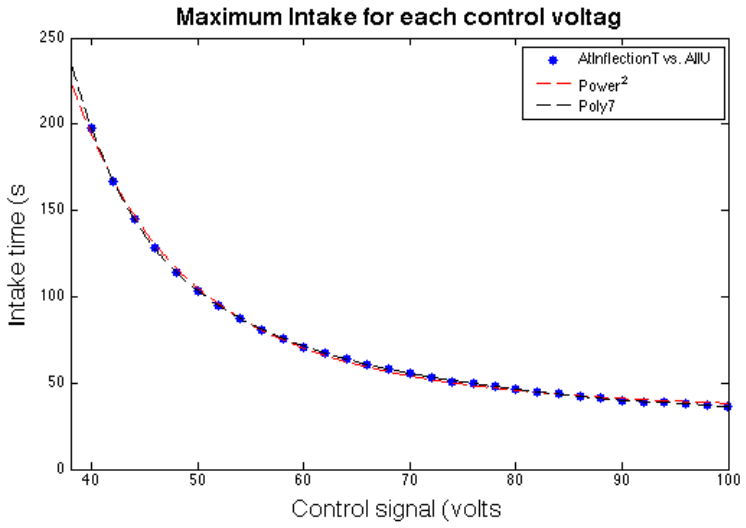

Figure 3.23: Fitting of the maximum intake without saturation of the left tank for each control percentage.

Using the equations presented in Table C.1, in appendix C, each percentage input can be used to verify if the current intake time is within the limits. Also, each intake time input can be compared with the maximum intake time allowed for the given percentage.

In either case, if the values are not within the limits, then the pop-up window will appear (Figure C.1.(a) in appendix C). The pop-up warns the user that a saturation is going to occur and offers a chance to auto-adjust the value.

The right most side of the configuration panel (Figure 3.21) provides the user with a option to choose how much time the drugs stay in the bloodstream, within a range starting at 622 s (30 s ingestion with a 2 V control voltage for $pump_1$) and 2813 s (900 s ingestion with a 2 V control voltage for $pump_1$).

Each curve of Figure 3.19.(a) between the green and red lines represents a curve in Figure 3.24 (the red curve corresponds to a 40_1 pump flow, the first percentage available in the option box). Using these curves, is possible to display to the user only the correct range of percentages for $pump_1$ for each input in the time in bloodstream form.

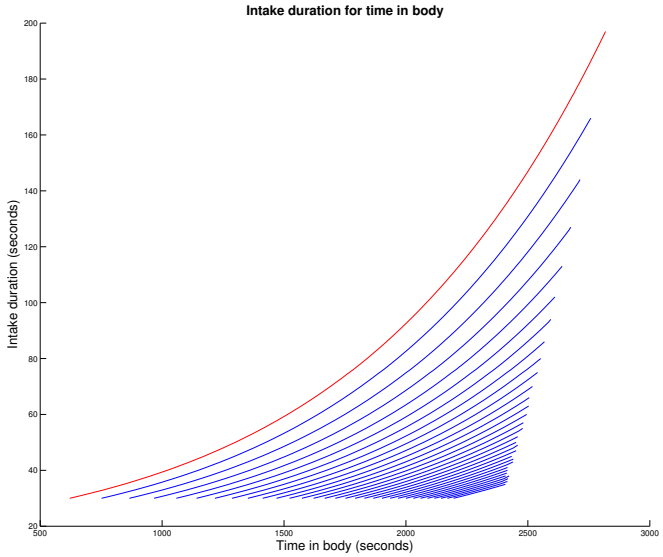

Figure 3.24: Curves representing the relation between ingestion time and time in bloodstream.

To find the relation between time in the bloodstream and the intake time for each of $pump_1$ percentages, each curve was fitted using a third order equation and is only used in the correspondent time intervals. The time intervals and fitting coefficients can be found in Table C.2, appendix C.

Using the parameters from Table C.2 in appendix C, it is possible to automatically calculate the intake duration for each pair time in bloodstream and the $pump_1$ percentage settings chosen.

A platform for simulate the intake of paracetamol (12 mg/kg) either in solution or in table was also developed and can be seen in Figure 3.25 as a screenshot of the platform.

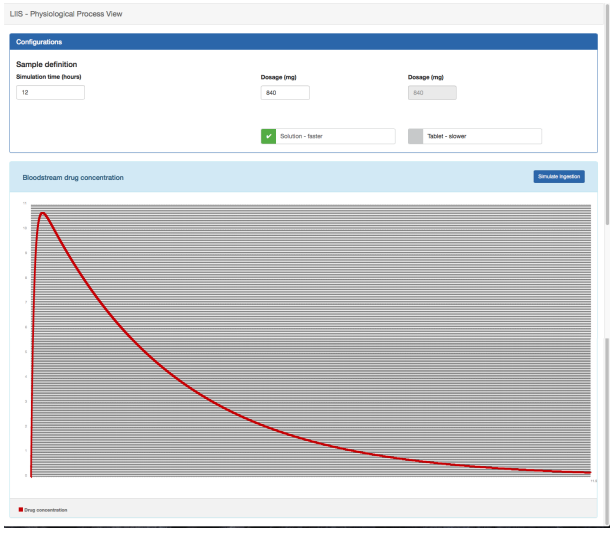

Figure 3.25: Web-based platform to simulate the ingestion of paracetamol.

3.3.2 Remote lab platform

After the platform for simulation was built and tested, the next step was to build the online interface that allows a user to simulate remotely an ingestion using the three-tank lab system. The platform to perform the online experiment can be seen in Figure 3.26.

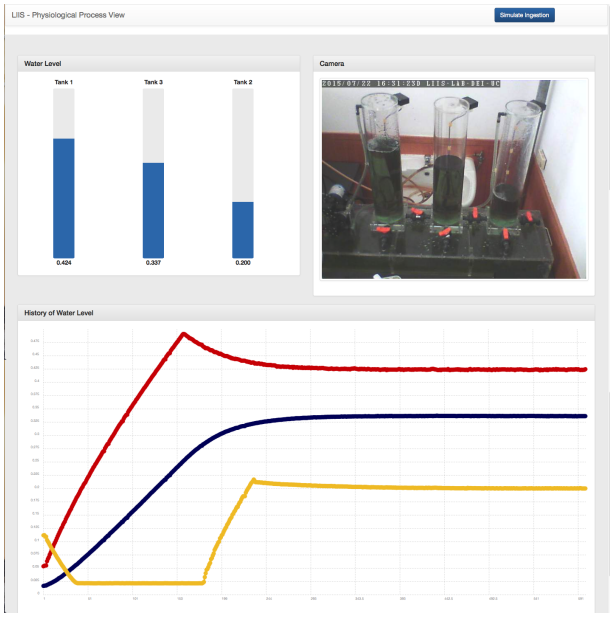

Figure 3.26: Screenshot of the remote platform for online experimentation.

The network component of the platform (communication with the data acquisition and actuator equipment and a first version of the online platform) was done in conjunction with the informatics engineering MSc. students Joaquim Leitão and Vitor Sousa.

In addition to the graphical representation of the water tanks level and its history, a live web-cam feed is also included, in order to compare the sensor data with the real water tanks level.

When the page is loaded, there is an initial setup to stabilize the water level in the tanks. After that ,the "Simulate ingestion" button is unlocked, and the user can simulate a single drug ingestion that happens 10 s after the button is pressed. It causes the value of $pump_1$ control voltage to change from 1.3 to 4 V for 35 s (ingestion period).

Also, the first time the user pushes the button establishes the centre tank threshold.

Figure 3.27: Snapshot from the webcam feed.

Figure 3.27 shows a snapshot from the webcam feed.

The valve between the left and the centre tank is open 75% and the exit valve from the centre tank is only open 25%.

It can also be seen that the centre tank is not coupled to the right tank, since the valve between both tanks is closed, isolating the right tank. The exit valve of the right tank is completely open.

The platform was successfully used at exp.at'15 conference, where an ingestion was simulated remotely. In Figure 3.28 presents a screenshot of two consecutive ingestions.

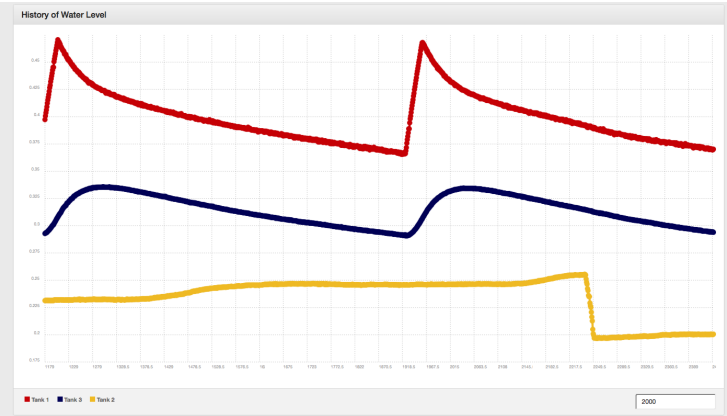

Figure 3.28: Screenshot showing the result of two consecutive ingestions.

3.3.3 Plot comparison and analysis

Both platforms provide similar responses when subjected to an ingestion of a drug. Their shape are very similar, providing a good indication that the simulated behaviour is a suitable alternative when the remote platform is unavailable, and that both controllers are working as expected. Also, the obtained results can be reshaped and converted into an approximation of a real drug ingestion, e.g Paracetamol.

The major difference between both platforms are the base levels and the right tank level behaviour.

Since the base level for the left and centre tanks are very dependent on the valve position, a small change in its angle produce a much different outcome on their levels. Without a smart controller for pump_1 or computer controlled valves, it can be sometimes difficult to replicate the experiments. These differences can cause different thresholds to be set with every experiment and influence the time window that allows for the perturbation to be passed upon the right tank, meaning that the time where the blue line in Figure 3.28 is above the threshold maybe very small, producing smaller quantities of water to be pumped into the right tank.

When talking about the right tank water level, small discrepancies between simulation using the computer and simulation using the three-tank process can occur. A possible explanation for these behaviours is the combination between a noisy signal (making it harder to find the peak in the centre tank), a high centre tank threshold (resulting in small quantities of water to be transferred to the right tank when an ingestion occurs) and/or an incorrect base level (causing either the left tank level to saturate similarly to Figure 3.19.(a)).

In Figure 3.28, when analysing the yellow line it can be seen the effects of the noisy data. The right tank level only starts to increase some time after the peak is past, an indication that the algorithm only found the downward slope in a region far from the peak. The downward slope is found by an algorithm that compares all 4 previous points to the current value and checks if all of them are higher than the current value (this comparison on starts after the ingestion peak is found). If the noisy signal produces a spike in any of these previous 4 points, then the pump_2 control signal is not increased, and, therefore, the level of the right tank is not changed.

The online platform worked as intended, being tested from a remote location without any communication problems and allowed several ingestions to be performed.

Chapter 4

Modelling the anaesthetic state using real data

In this chapter a model that relates physiological input variables with the bi-spectral index was developed.

Unfortunately, the system used to compute BIS is prune to some interferences. In our study, the datasets have large intervals of time without data for the BIS, probably from electrical interference when using an electrical scalpel or a low signal quality.

The following sections describe the steps taken and the conclusions obtained in the modelling of the anaesthetic state from real data. It was tried to use state-of-the-art variables (measures) returned by the surgery room instrumentation that are less prone to interferences.

4.1 Datasets

The datasets used in this thesis were obtained in a previous work [56]. These datasets are made up of several physiological measures recorded during seven different surgical procedures. For five of those seven surgeries there are informations about sex, age, type of procedure and a timeline describing events that occurred.

4.1.1 Variables (measures)

From the list of 46 measures, only 21 plus the BIS are used in this context. The 21 parameters are recorded by the anaesthesia station Dräger Fabius Tiro, while the BIS is calculated by the sensor BIS QUATRO from Aspect Medical Systems, Inc.

Table 4.1 describes the measures recorded by the anaesthesia station mentioned above.

Table 4.1: Measures recorded by the anaesthesia station Dräger Fabius Tiro.

HR	Heart rate	**SpO_2**	Pulse oxygen saturation	**PLS**	Pulse
$etCO_2$	Dioxide carbon final expiration pressure	**iCO_2**	Dioxide carbon inspiration	**PIP**	Positive inspiration pressure
RRc	Respiration rate	**PEEP**	Positive expiration pressure	**MAP**	Mean arterial pressure
MVe	Minute ventilation	**TVe**	Total ventilation	**RRv**	Respiration rate
NBPS	Systolic arterial pressure	**NBPD**	Diastolic arterial pressure	**NBPM**	Mean arterial pressure
iO_2	Oxygen inspiration	**etO_2**	Final oxygen expiration pressure	**etSEV**	Final sevoflurane expiration pressure
iSEV	Final sevoflurane inspiration pressure	**etN_2O**	Final nitrogen expiration pressure	**iN_2O**	Final nitrogen inspiration pressure

4.1.2 Drugs and intervals

To better analyse each one of the datasets, when information was available, a three stage time splitting was implemented, based on annotations taken during the surgery. The three sub-parts include data related to the conscience falling, anaesthesia maintenance and conscience recovering.

Statements similar to 'Start of surgery' or 'Start' were used to mark the change from a conscience falling to an anaesthesia maintenance state, while statements in line with 'End of surgery' or 'End' were used to mark the change from an anaesthesia maintenance to a conscience recovering state.

For the datasets patient8 and patient9, no information was available.

Based on all the notes available, approximately ten different drugs were used. They were: Atropine, Cetorolac, Cisatracurium, Droperidol, Fentanil, Metilprednisolona, Ondansetron, Rocuronium, Sevoflurane and Tiopental. In appendix D, a list of effects and usage for each drug can be found, while appendix E a description about the relation between drugs and the datasets is provided.

Since the quantity of information in how or why those drugs were administered is very limited, the influence of drugs is discarded.[1]

Table 4.2 contains the different intervals found during the analysis of the procedure notes.

[1]Except for Sevoflurane, since the administration can be measured by two of the recorded measures (etSEV and iSEV).

Table 4.2: Periods during surgery related to the conscience falling, anaesthesia maintenance and conscience recovering. Each time is in minutes and is relative to the beginning of the surgery.

Data set	Conscience falling	Anaesthesia maintenance	Conscience recovering
Patient3	12 - 51	52 - 409	410 - 420
Patient4	04 - 22	23 - 68	69 - 81
Patient5	22 - 54	55 - 133	134 - 140
Patient7	06 - 25	26 - 85	86 - 89
Patient10	00 - 19	20 - 95	96 - 106

4.1.3 Missing data and imputation

The first analysis performed on the datasets was to assess their quality. One metric that can be used to study each measure is the amount of data that is missing for each dataset. If a measurement has to many missing values, it should not be further used since conclusions drawn from such measurement (even after imputation) may not represent the truth.

Table 4.3 provides the values in percentage of the missing values for each measure for each data set. The green colour represents values between 0% and less than 15%, yellow colour represents values from 15% and less than 75% and the values with colour red between 75% and 100%.

The next question is what percentage of missing data should be the limit between reasonable missing values and excessive quality loss. The problem in defining this limit resides on the high values of missing values for the BIS, with the highest being 52% and the lowest 28%, with an average of 38%. If the highest of the values mentioned before is taken, then only three measures were to be excluded from all datasets, while using lower values entails removing complete datasets.

Taking in account the low number of datasets available for analysis, the only excluded measures were the systolic, diastolic and mean arterial pressures (NBPS, NBPD, NBPM), with an average of 80% of missing values for each dataset.

The same analysis can be extended to each interval. To compare the results from each segment, table 4.4 consists of the averages for each interval. The green colour represents values between 0% and less than 15%, yellow colour represents values from 15% and less than 75% and the values with colour red between 75% and 100%.

Table 4.3: Missing value percentages for each measure for each dataset.

Variable	Patient3	Patient4	Patient5	Patient7	Patient8	Patient9	Patient10
HR	0%	0%	5%	1%	1%	2%	1%
SpO_2	2%	0%	13%	2%	1%	2%	2%
PLS	2%	0%	13%	2%	1%	2%	2%
$etCO_2$	0%	0%	3%	1%	0%	2%	0%
iCO_2	0%	0%	3%	1%	0%	2%	0%
RRc	6%	15%	20%	16%	6%	12%	16%
PIP	0%	0%	3%	1%	0%	2%	0%
PEEP	2%	9%	12%	15%	3%	5%	3%
MAP	0%	0%	3%	1%	0%	2%	0%
MVe	0%	0%	3%	1%	0%	2%	0%
TVe	0%	0%	3%	1%	0%	2%	0%
RRv	5%	16%	19%	13%	6%	15%	14%
NBPS	80%	78%	81%	80%	81%	80%	80%
NBPD	80%	78%	81%	80%	81%	80%	80%
NBPM	80%	78%	81%	80%	81%	80%	80%
iO_2	0%	0%	3%	1%	0%	2%	0%
etO_2	0%	0%	3%	0%	0%	2%	0%
etSEV	0%	0%	3%	0%	0%	2%	0%
iSEV	0%	0%	3%	0%	0%	2%	0%
etN_2O	0%	0%	3%	0%	0%	2%	0%
iN_2O	0%	0%	3%	0%	0%	0%	0%
BIS	28%	30%	43%	41%	52%	32%	38%

When reviewing Table 4.4, the percentages of missing data per measure are very similar among all the intervals, with the exception of measures in the conscience falling phase. However, this phase is not crucial to this research, since maintaining a stable value of the BIS during surgery is the mentioned benefit of using the BIS.

For the retained measures, some type of data imputation was needed if further analysis was to be conducted on them. Based on the supported past thesis [56] and the assumption that during anaesthesia the rate of change of each measure should be very low, a linear interpolation was chosen as the data imputation method.

Linear interpolation, equation 4.1, uses two consecutive points ((x_0,y_0) and (x_1,y_1)) to derive a straight line between them and subsequently use it in order to get the values in missing (x,y).

$$y(t) = y_0 + (x - x_0) * \frac{y_1 - y_0}{x_1 - x_0} \tag{4.1}$$

Table 4.4: Missing value average percentages for each measure for each interval.

Variable	Full duration	Conscience falling	Anaesthesia maintenance	Conscience rising
HR	1%	1%	0%	0%
SpO_2	3%	4%	2%	0%
PLS	3%	4%	2%	0%
$etCO_2$	1%	0%	0%	0%
iCO_2	1%	0%	0%	0%
RRc	13%	40%	0%	0%
PIP	1%	0%	0%	0%
PEEP	7%	12%	1%	2%
MAP	1%	0%	0%	0%
MVe	1%	0%	0%	0%
TVe	1%	0%	0%	0%
RRv	13%	36%	0%	0%
NBPS	80%	79%	79%	79%
NBPD	80%	79%	79%	79%
NBPM	80%	79%	79%	79%
iO_2	1%	0%	0%	0%
etO_2	1%	0%	0%	0%
etSEV	1%	0%	0%	0%
iSEV	1%	0%	0%	0%
etN_2O	1%	0%	0%	0%
iN_2O	0%	0%	0%	0%
BIS	38%	26%	38%	13%

More complex data imputation methods could have been used, but taking in account the considerations made above using this method should be enough at this stage of the analysis. The method described was applied using a Python script and the results can be seen in Figures 4.1 and 4.2. Two Python libraries were used, *matplotlib* for plotting the results (`http://matplotlib.org`) and *scipy* to perform the correlation described in subsection 4.2.1 (`http://www.scipy.org`).

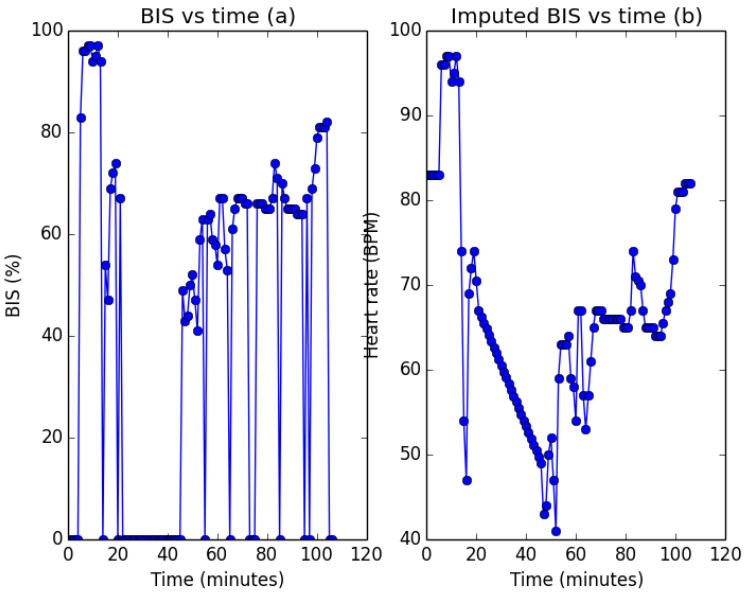

Figure 4.1: The BIS before (a) and after (b) the imputation. Data from patient10 dataset.

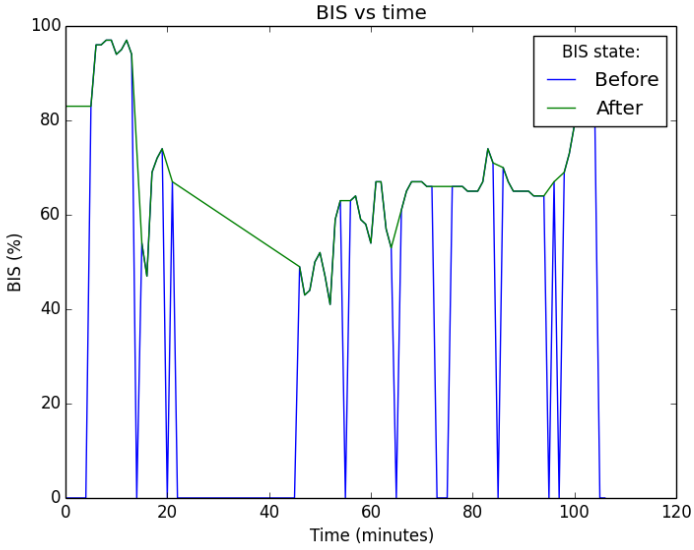

Figure 4.2: The BIS before (blue) and after (green) the imputation. Data from patient10 dataset.

In Figure 4.1.(a), it can be seen the effects of missing values. For some periods of time, for example from 20 to around 45 min (from the beginning of surgery), there is a jump from a certain percentage to zero, leaving a big window without any information about the BIS. By using linear interpolation, a more smooth representation of the data can be established in order to get a better picture of the anaesthesia evolution. Figure 4.2 compares the original data with the imputed data by overlaying the two datasets.

In Figure 4.3 a difference in missing data intervals can be seen. While the BIS has 41 points missing, the HR only have one. During the interval between 20 and 45 min, there is no value for the BIS and it had to be imputed. However, during this period it can be seen in Figure 4.3.(b) that the HR had some variation. When analysing this time window, it shows that the value for the BIS is decreasing linearly while, in this case, the HR is having changes, possibly affecting the correlation values for this period window.

Given that all datasets available have a moderate level of missing data for the BIS, there is no real solution to this problem.

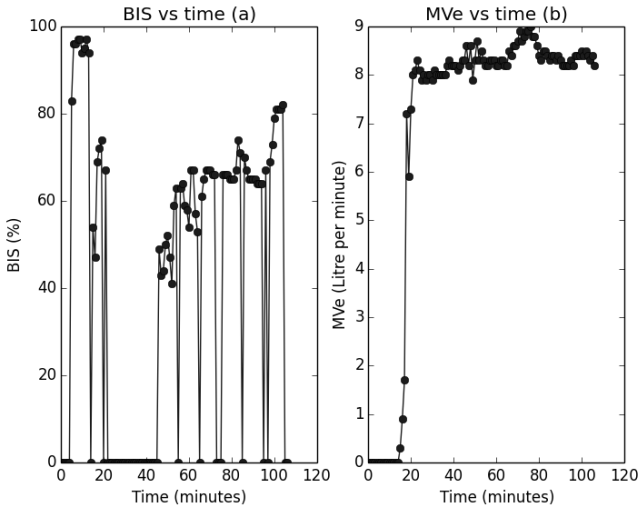

Figure 4.3: BIS vs time (a) and HR vs time (b). Data from patient10 dataset.

4.2 Dataset Analysis

4.2.1 Correlations with BIS - Global and by intervals

After discarding measures with low amount of information and imputing values for the remaining[2], a Pearson correlation test between all measures and the BIS was made, in order to select the measures that best meet the requirements to establish a predictor for the BIS.

First, all the selected measures were correlated with the BIS for the entire duration of each data set. If the correlation value between a measure and the BIS was higher than or equal to 0.5 or less than or equal to -0.5, the measures were deemed correlated (appendix F includes the correlation tables for each data set; rule 4.1 is a more comprehensive overview of the rule mentioned). The same was performed using the intervals described in Table 4.2.

[2]Although the correlations should have been done with the raw datasets, their results from these correlation were all zero. Instead of stop the search for any relation, it was decided to perform the correlation after imputing the missing values.

Rule 4.1 Rules to consider if a measure is or is not correlated to the BIS

if -0.5 $\leq$ Correlation between a measure and the BIS $\geq$ 0.5 **then**
Measure is correlated in this dataset (1)
else
Measure is not correlated in this dataset (0)
end if

Table 4.5 is constructed by applying rule 4.1 on the four different time intervals on all the available datasets. The red colour represents values between 0% and less than 25%, orange colour represents values from 25% and less than 50%, yellow colour represents values from 50% and less than 75 percent and the values with colour green between 75% and 100%.

Table 4.5: Correlation between measures and the BIS in different time intervals.

Variable	Full duration	Conscience falling	Anaesthesia maintenance	Conscience rising
HR	29%	40%	0%	60%
SpO_2	29%	20%	0%	40%
PLS	29%	40%	0%	60%
$etCO_2$	71%	40%	20%	40%
iCO_2	0%	0%	0%	20%
RRc	86%	20%	0%	60%
PIP	71%	60%	0%	40%
PEEP	86%	40%	0%	40%
MAP	71%	80%	20%	20%
MVe	100%	60%	20%	60%
TVe	100%	40%	20%	40%
RRv	57%	20%	0%	40%
iO_2	71%	20%	20%	80%
etO_2	57%	0%	20%	60%
etSEV	71%	20%	40%	80%
iSEV	71%	20%	40%	80%
etN_2O	0%	0%	20%	20%
iN_2O	0%	0%	20%	20%

Each measure of each dataset returns a binary value. All binary values from each dataset are summed and the sum is divided by the number of datasets. This operation gives for each measure the percentage of occurrence in all dataset.

For example, the MVe measure is correlated with the BIS in all datasets (7 out of 7) when considering the full duration interval, but is correlated in 60% of the datasets (3 out of 5) when considering the conscience falling interval.

Again, the need to define a threshold emerges. When analysing the anaesthesia maintenance column in Table 4.5, the highest correlation value is 40% (etSEV and iSEV) while most values are either 0, 20 or higher than 40%.

Taking this in account, the threshold established was equal or higher than 40% in order to include at least one measure in the anaesthesia maintenance interval. When studying the effects of sevoflurane (appendix D), one can argue that the value for the BIS is correlated to the expired and inspired pressure of sevoflurane since it used to maintain the general anaesthesia during surgery.

Using the threshold of 40%, Table 4.6 contains the measures that are taken as correlated with the BIS for each interval.

Table 4.6: Variables that are 40% or higher percent correlated with the BIS.

Full duration	$etCO_2$, RRc, PIP, PEEP, MAP, MVe, TVe, RRv, iO_2, etO_2, etSEV, iSEV
Conscience falling	PIP, PEEP, MAP, MVe, TVe
Anaesthesia maintenance	etSEV, iSEV
Conscience rising	HR, SpO_2, PLS, $etCO_2$, RRc, PIP, PEEP, MVe, TVe, RRv, iO_2, etO_2, etSEV, iSEV

There is not a single measure that is common in all 4 intervals, being the most frequent measures appearing the PIP, PEEP, MAP, MVe, TVe, etSEV and iSEV, present in 3 out of 4 intervals.

4.2.2 Correlation between the selected measures

Having established what measures are correlated for each interval, the following step is to ascertain the correlations between themselves. If two measures are highly correlated, one can be discarded since the is not a high gain in information.

For example, when considering the full duration interval there is a high number of measures that are correlated with the BIS, twelve to be precise. Out of this 12, there are measures that appear in pairs (for example iO_2, etO_2) and therefore are correlated.

Tables in appendix G provide a correlation per interval of the measures in study using rule 4.1. The following tables only show a reduced view about the number of cross-correlations.

Table 4.7 refers to the correlation between measures using the full duration of the procedure, while Table G.1 in appendix G represents the values for the correlations.

Table 4.7: Number of measures correlated with each measure for the full duration of the procedure.

$etCO_2$	RRc	PIP	PEEP	MAP	MVe	TVe	RRv	iO_2	etO_2	etSEV	iSEV
9	10	8	8	9	11	10	3	5	6	10	10

The measure that is most independent, i.e that has fewer measures correlated with, is the RRv, while the most dependent is the MVe, having a correlation with all the measures.

Based in this results, three different actions can be taken: select the MVe as the only measure to establish a relation with the BIS; select a number of measures that are the most correlated; or select a number of measures that are the least correlated to form the relation with the BIS.

The first proposal (using only one measure to establish a relation) is to some degree ill-advised. By using only one measure, the prediction of the BIS is very susceptible to interferences or errors that occur during surgery, even if in all datasets the MVe is well correlated with the BIS.

To minimize the number of errors influencing the prediction of the BIS, a higher number of measures can be used. By using a higher number of measures, the dependence of the prediction of each individual measure is lower. The challenge then is to establish how to select the best measures: on the one hand, the selection of the measures with the highest number of correlations (proposal two), on the other hand, the selection of the measures with the lowest number of correlations (proposal three).

If the measures with the highest number of correlation are selected (proposal two), they can be combined to supplant the non-correlated measures between them. For example, one can select MVe, TVe and RRc. As mentioned before, the MVe is correlated with all the measures so it should be included in this line of though. Inspecting the TVe, the only uncorrelated measures is the RRv, but the RRv is one of the most uncorrelated measures. So instead of including the RRv, the RRc is chosen, since is one of the measures that is most correlated with the remainder and is correlated with the RRv.

Taking now the option that considers the lowest number of correlations (proposal three), the same principle of supplanting the measures missing applies. The measure to be selected is the one that least correlates with the rest of the candidates, in this case the RRv. This measures does not correlate with the following: PIP, PEEP ,MAP, TVe, iO_2, etO_2, etSEV, iSEV. RRv only correlates with two out of the other eleven candidates.

From the list of non correlating measures with RRv, iO_2 is the next measure with the lowest number of cross correlations. The measure that are not correlated with iO_2 are: PIP, PEEP, MAP.

Out of this three, the PIP and the PEEP both have the same number of correlated measures (eight) and both correlate with the MAP (which has nine correlated values). However the PIP has a higher correlation value with MAP, having the potential for a better choice than the PEEP.

In short, in order to avoid complexity and still have enough measures to be used in estimating a value for the BIS, two different path can be followed. The first is selecting the measures that are most correlated with the others, in this case the MVe, TVe and RRc. The second option is the opposite, the selected measures are those that have the lowest number of correlated measures, in this case the RRv, iO_2 and PIP.

The next step was to analyse the correlations within the three considered intervals. Tables 4.8, 4.9 and 4.10 show the number of correlated measures for each measure for each interval.

Table 4.8: Number of measures correlated with each measure for the conscience falling interval.

PIP	PEEP	MAP	MVe	TVe
1	3	4	3	3

Table 4.9: Number of measures correlated with each measure for the anaesthesia maintenance interval.

etSEV	iSEV
1	1

Table 4.10: Number of measures correlated with each measure for the conscience rising interval.

HR	SpO_2	PLS	$etCO_2$	RRc	PIP	PEEP	MVe	TVe	RRv	iO_2
2	0	2	2	1	2	1	2	1	0	0
etO_2	etSEV	iSEV								
1	1	1								

For the conscience falling, since there are only four measures, all can be used in finding a connection with the BIS. In appendix G, table **??** shows the correlation values between all the measures included in this interval.

The same applies for the anaesthesia maintenance interval, since there is are only two measures that are correlated with each other. Table G.3 in appendix G shows the correlation between themselves.

The last interval is different than the rest (Table G.4 in appendix G). There are multiple measures that are uncorrelated among them. For this interval, the measures chosen should be the ones that are not correlated with any other plus, a selection of the correlated measures. Accordingly, the measures for this interval are: SpO_2, RRv, iO_2 (zero correlation with the rest of the measures), PLS (between HR, PLS and PIP, PLS has the highest correlations), $etCO_2$ (correlates with RRc and etO_2), MVe (correlates with PEEP and TVe), either etSEV or iSEV (they are correlated between them only).

Table 4.11 is a list of the measures that are potential candidates to have a relation with the BIS using correlation tests for each interval.

Table 4.11: Variables that are selected as potential candidates to have a relation with the BIS.

Full duration	MVe, TVe, RRc or RRv, iO_2 and PIP
Conscience falling	PIP, PEEP, MAP, MVe, TVe
Anaesthesia maintenance	etSEV or iSEV
Conscience rising	SpO_2, PLS, $etCO_2$, MVe, RRv, iO_2, etSEV or iSEV

4.3 Model development

To develop a model that can relate the variables found in Table 4.11, two different modelling strategies were used: a multivariable and a multivariate. This two models are used in medicine for data description and inference [73].

A multivariable model, also known as multiple linear regression, can be thought of as a model in which multiple variables are used to predict an outcome [74]. The equation representing this model is equation 4.2,

$$y = \alpha + x_1\beta_1 + x_2\beta_2 + \ldots + x_i\beta_i \tag{4.2}$$

where y is the continuous variable to be predicted, $x_1, \ldots, x_i$ are multiple predictors, $\beta_1, \ldots, \beta_i$ the coefficients for the multiple predictors and α a constant.

A multivariate model, by contrast, refers to the modelling of data that are often derived from longitudinal studies, where an outcome is measured for the same individual at multiple time points (repeated measures, in this case the BIS values throughout the surgery) [74]. The equation representing this model is equation 4.3,

$$Y_{n\times p} = X_{n\times(k+1)}B_{n\times(k+1)} \tag{4.3}$$

where Y is the continuous variable to be predicted, X is a matrix with the multiple predictors and B the matrix coefficients for this predictors.

This type of model is normally used with multiple outcomes for the dependent variable Y, but since for each patient it is only available one outcome, the model was developed with only one possible outcome.

In theory, a multivariate model should have a better performance than a multivariable model since it assumes that the values for the predictors are taken in different time intervals for the same individual.

4.3.1 Variables used

Based on table 4.11, the variables used to build the models were the MVe, the TVe, the RRc and the iSev.

For each dataset, only the values when the BIS was different of 0% were used. Figure 4.4 represents the scatter plot for each variable against the BIS from all datasets.

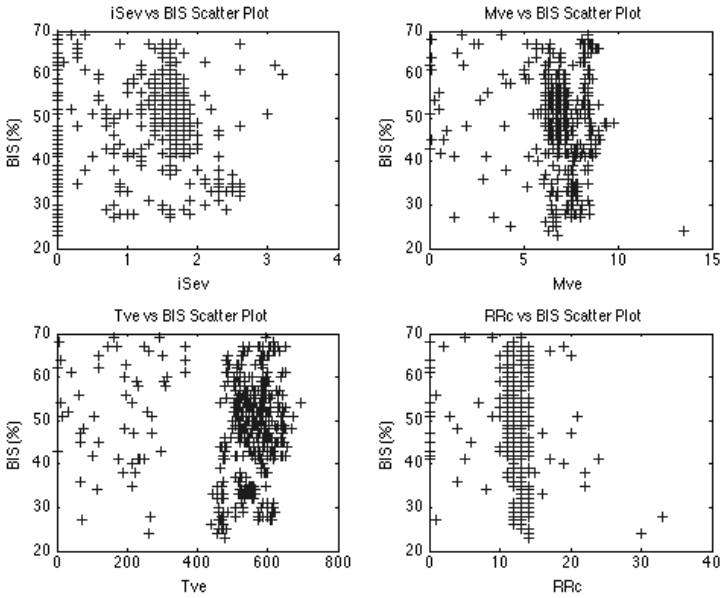

Figure 4.4: Scatter plots for the variables versus the BIS.

In each of the variables scatter plots, it is visible the presence of clusters of points. The existence of these clusters is not ideal, since it represents that for multiple values of the BIS the value of the predictor is the same and vice-versa. An ideal situation would have been a linear[3] distribution of the predictors.

Although individually the variables would not be ideal for the development of a model, using a combination of them could produce a better result.

These higher dimension models were developed using the *mvregress* function in MATLAB for the multivariate models and the *LinearModel.fit* function for the multivariable models.

4.3.2 Model development

For each dataset, a multivariate model and a multivariable model were developed. The root mean square error (RMSE) between the BIS and the prediction was calculated as a performance indicator.

[3]Or non-linear if non-linear models were to be developed

Table 4.12 is the RMSE values for each model for each dataset.

Table 4.12: RMSE value for each model for each dataset.

Dataset	Multivariate RMSE (%)	Multivariable RMSE (%)
Patient3	8.87	6.44
Patient4	23.93	12.00
Patient5	24.23	9.27
Patient7	18.71	9.25
Patient8	25.66	12.44
Patient9	37.09	10.99
Patient10	36.59	9.35

An interesting result can be seen when analysing the results obtained for the RMSE values: the RMSE values for the predictions done using a multivariate model are higher than those obtained by using a multivariable model. The expected outcomes were lower RMSE values when using a multivariate model, since it takes into account that the predictions are for the same individual taken at a different times.

In Figure 4.5 it can be seen, for patient3 dataset, the prediction for the BIS using the two different models.

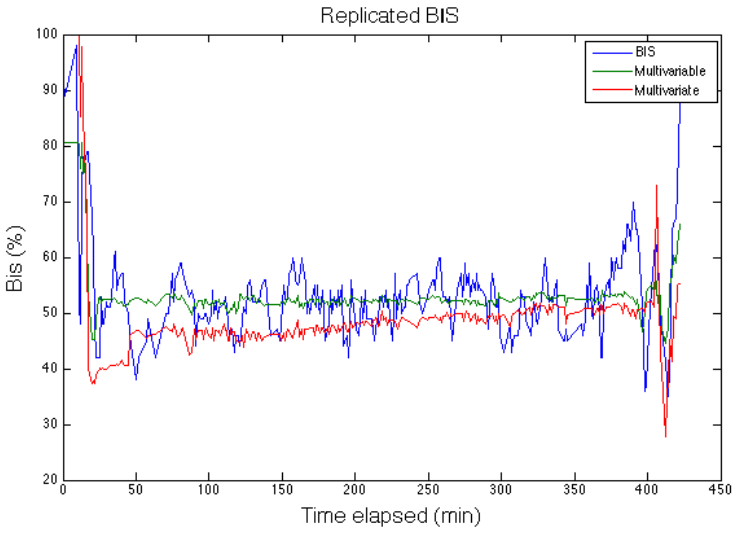

Figure 4.5: The BIS and predictions it using the two different models. (patient3 dataset)

During the anaesthesia maintenance interval, the value for the BIS and the predictions are similar. Since this is also the interval of most interest, for the datasets containing the information about the intervals two new multivariable and multivariate models were developed. Table 4.13 is the RMSE values for each model for each dataset.

Table 4.13: RMSE value for each model for each dataset in the anaesthesia maintenance interval.

Dataset	Multivariate RMSE (%)	Multivariable RMSE (%)
Patient3	5.68	5.14
Patient4	6.22	4.91
Patient5	4.01	3.78
Patient7	6.85	2.05
Patient10	9.94	6.21

When the models are developed and tested using only data from the anaesthesia maintenance interval, the RMSE values are lower for both models when comparing with the full dataset. In each of the five datasets used, the values for the RMSE in both models are lower than 10%, being the averages 6.83 and 4.39% for the multivariate and the multivariable model respectively.

In Figure 4.6 it can be seen, for patient3 dataset, the prediction for the BIS in the anaesthesia maintenance interval using the two different models.

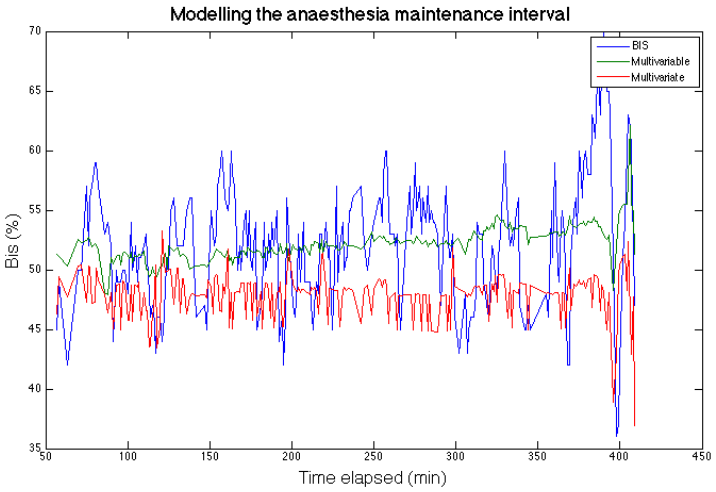

Figure 4.6: The BIS and predictions using the two different models for the anaesthesia maintenance interval. (patient3 dataset)

In Table 4.14 the values for the coefficients of each model are presented.

Table 4.14: Models coefficients

Dataset	Multivariate model				Multivariable model				
	B_1	B_2	B_3	B_4	α	β_1	β_2	β_3	β_4
patient3	14.168	-0.162	1.752	12.012	16.364	13.540	-0.136	2.021	13.435
patient4	9.199	-0.084	1.743	-7.347	85.630	-4.523	0.018	-1.988	3.050
patient5	27.137	-0.205	-1.012	-19.792	111.731	14.848	-0.227	-2.194	-16.459
patient7	-49.201	1.040	-8.306	0	69.933	-7.007	0.085	-1.168	0
patient10	-9.181	0.164	4.768	-13.449	48.010	-6.789	0.096	2.331	-10.794

4.3.3 Validation

Since there are two datasets (patient8 and patient9 datasets) out of the seven that are not divided by intervals, they can be used to asses the performance of each of the models in new data.

Although there are no notes for theses two datasets, from the analysis of their curves an interval for each dataset can be determine. The following Tables 4.15 and 4.16 contain the RMSE values for each model developed from the other datasets.

Table 4.15: RMSE for dataset patient8 using the models from the other datasets.

Dataset	No interval		Interval (Elapsed time <65 min)	
	Multivariate RMSE(%)	Multivariable RMSE (%)	Multivariate RMSE (%)	Multivariable RMSE (%)
patient3	29.09	19.08	11.10	25.94
patient4	31.32	14.80	11.25	7.65
patient5	42.03	31.37	34.62	38.51
patient7	28.99	25.93	9.23	33.87
patient10	40.50	33.93	44.23	43.47
Means	34.39	21.42	21.93	29.89

Table 4.16: RMSE for dataset patient9 using the models from the other datasets.

Dataset	No interval		Interval (Elapsed time <25 min)	
	Multivariate RMSE(%)	Multivariable RMSE(%)	Multivariate RMSE(%)	Multivariable RMSE(%)
patient3	39.67	28.17	16.85	34.63
patient4	40.61	13.90	17.29	17.09
patient5	54.86	44.53	44.12	49.27
patient7	38.20	36.20	13.14	44.21
patient10	54.48	43.64	51.21	50.48
Means	39.56	33.29	28.52	39.14

4.4 Discussion

Figure 4.7 is the plot of the BIS predictions for patient8 and patient9 datasets made by the models developed using patient7 dataset.

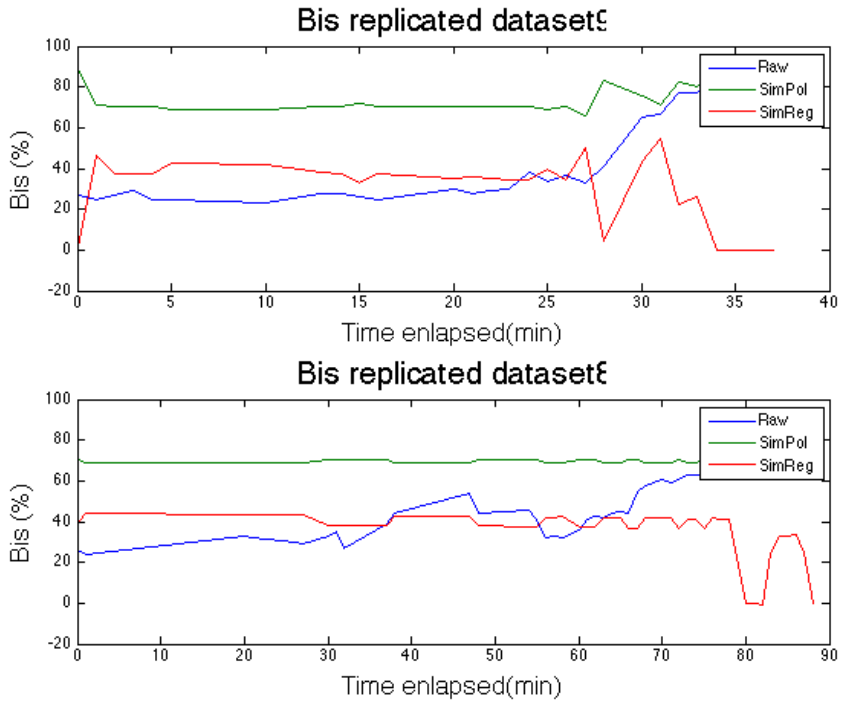

Figure 4.7: Patient7 dataset model validation.

As mentioned before, the predictions made using the multivariable model should be closer in value to the BIS than predictions made by the multivariate model, since their RMSE values are lower.

But when analysing figure 4.7, this seems not to be the case. The green line (representing the prediction made using the multivariable model), for the values between 0 and 65 min of elapsed time, have a much higher value than the prediction made by the multivariate model (red line). The usage of an time interval arises from this fact, since this situation occurs in almost all the datasets.

When comparing the values for the RMSE inside the time interval, it can be seen that generally the multivariate models have a lower error values. This could be due to the α value of the multivariable model for each dataset. The lowest value for α is 16 while the highest is 111, with a standard deviation of this value is 36.33. This big range of value for alpha make each model very dataset dependent.

For the multivariate models, the datasets patient3, patient4 and patient7 had low values for the RMSE when an time interval was considered, with the best result being the model developed from patient7 dataset when comparing with patient 8 dataset.

A possible reason for the values of patient9 dataset RMSEs being higher than the values of patient8 RMSE could be the number of points (28 points) to predict and compare.

The BIS has a range of 0 to 100% with a value below 60% being associated with a low probability of response to commands by a patient under anaesthesia [75]. When analysing the values of the RMSE, their averages have a high value (above 20%), representing a third of the scale between 0 to 60%. Therefore, these models do not represent good enough predictors of the BIS if used in a clinical environment.

Although they do not predict the BIS with a good enough performance, they show that a relation with the BIS can be obtained.

Chapter 5

Conclusions and future work

The intent of this thesis was to develop physiological models using two different approaches, a computational and a hybrid.

Due to the available resources and the state of the art, the following models were initially considered: use of a database developed last year to try to find knowledge regarding liver injuries; use a three-tank control process to remotely simulate the ingestion, propagation and excretion of a drug; and use datasets from surgeries to find a relation between the BIS and other physiological variables.

Out of this three main objectives initially considered, the liver modelling was dropped once it was not possible to build a problem description and safely access the platform. From the both meetings that were conducted with physicians from Internal Medicine A of the CHUC, an interest from both parties was clear but scheduling and communication difficulties prevented a clear understanding of the problems and what it would have been interesting to look for in the database.

The next sections contain some conclusions and future work for each of the models developed.

5.1 Hybrid Model

Two different web apps were developed that allow a user to either use the online experiment or use an offline simulation, being the platforms compared to a real life scenario of ingesting a 12 mg/kg tablet of paracetamol.

Although a remote simulation of a drug ingestion can be performed, the platform has some limitations, that can be considered for future work.

An improvement to be done is to give the user more configuration options, in pair with the options offered in the simulated ingestion. At this stage, the user can only decide when to simulate and has no control of the duration and pump flow variation. Also a field to display the threshold value in order to assess if it is high or low, and the corresponding option to increase and decrease accordingly are advised.

Both the left and centre tanks could have a controller for the base level. Every time the experiment is carried out, there are two valves that have to be set, and since there is no electronically controlled valves there is a margin of error when setting the angles of the valves.

Since the base level is only controlled by a constant flow, any change in the valve angle is not corrected or taken into account, causing the experiment to be very hard to replicate. In order to correct this problem, a water level based controller for pump_1 or electronically controlled valves would be need.

To improve the model, the outflow valve in the left tank should be partially open to model the metabolic losses and the quantity of drug that is not absorbed by the bloodstream. The angle of this valve can be determined if a drug bioavailability percentage is known.

The offline platform allows a better control of the parameters. There are some limitation with this platform, mainly the tendency to consume a large amount of RAM if the web browser tab is not closed.

Another feature that should be implemented is an integration of experimental protocols and reporting it in the platform, similar with what is done in [51], where students can consult different experimental protocols to be accomplished using the remote lab and upload reports with their findings.

In conclusion, although there are some improvements to be done to the platform and the tank architecture imposes some limitations when building an equivalent model for the process in study, an equivalent model based on a three-tank process for an ingestion, propagation and excretion of a drug was developed and, more specifically, the ingestion of a 12 mg/kg tablet of Paracetamol can be remotely simulated using the equivalent model developed. The usage of this platform as a teaching aid, especially in the biomedical field, provides a visual stimulus and a practical example of the implementation of equivalent models when studying physiological systems.

Also the usage of the three-tank process in a two plus one configuration, simulating a physiological process is, to the best of the author knowledge, a new approach for this system and demonstrates the versatility of reusing control systems in modelling physiological systems.

5.2 Anaesthesia Model

The main objective of this model was to establish a relation between some measured physiological variables and the BIS. Two different type of models were used: a multivariate and a multivariable.

The analysis conducted has the assumption that the values during the intervals that were not registered did not change in a drastic manner. The data acquisition of one sample per minute can also hide any fast change in patient status or any indicator. Also, the

available datasets did not have information about abnormal events.

From 10 different obtained models (2 per each of the 5 dataset that were divided by intervals), the multivariate models had a lower root mean square error when comparing with the multivariable models in the validation datasets patient8 and patient9.

The error means were (for the multivariate model) 36.98% outside the intervals and 25.23% inside. Since the BIS has a range of 0% (EEG silence) to 100% (awake) and a value between 40 and 60% indicates an appropriated level for general anaesthesia [76], those values are to high to be used with confidence in a clinical environment.

Although these models has some limitations, they show that a relation with the BIS and other physiological variables can be obtained.

Future work should include the usage of better datasets and the accompaniment of a physician in order to validate the candidate lists obtained (Table 4.11). Also the models should be tested using more datasets and their prediction should be compared with real-time BIS values.

References

[1] J. Kretschmer, T. Haunsberger, E. Drost, E. Koch, and K. Möller, "Simulating physiological interactions in a hybrid system of mathematical models," *Journal of clinical monitoring and computing*, vol. 28, no. 6, pp. 513–523, 2014.

[2] R. P. van Wijk van Brievingh and D. P. F. Möller, eds., *Biomedical Modeling and Simulation on a PC: A Workbench for Physiology and Biomedical Engineering*, vol. 6: Advances in simulation, ch. 1 and 2, pp. 1–7 and 45. Springer, 1993.

[3] S. R. Devasahayam, *Signals and Systems in Biomedical Engineering: Signal Processing and Physiological Systems Modeling*, ch. 14, p. 312. Springer, 2000.

[4] D. H. Anderson, *Compartmental Modeling and Tracer Kinetics*, ch. 1, pp. 2–8. Springer, 1983.

[5] I. G.-S. Partner, *DTS200 Three-Tank-System*. Ingenieurbüro Gurski-Schramm Partner, 2004.

[6] L. Z. Benet, D. Kroetz, L. Sheiner, J. Hardman, and L. Limbird, "Pharmacokinetics: the dynamics of drug absorption, distribution, metabolism, and elimination," *Goodman and Gilman's the pharmacological basis of therapeutics*, pp. 3–27, 1996.

[7] I. Khurana, ed., *Essentials of Medical Physiology*, ch. 6 - Excretory System, p. 339. Elsevier India, 2008.

[8] L. E. Gerlowski and R. K. Jain, "Physiologically based pharmacokinetic modeling: principles and applications," *J. Pharm. Sci*, vol. 72, 1983.

[9] B. Gholami, J. M. Bailey, M. Haddad, and A. R. Tannenbaum, "Clinical decision support and closed-loop control for cardiopulmonary management and intensive care unit sedation using expert systems," *Control Systems Technology, IEEE Transactions on*, vol. 20, no. 5, pp. 1343–1350, 2012.

[10] C. Cobelli and E. Carson, *Introduction to modeling in physiology and medicine*. Academic Press, 2008.

[11] T. Eissing, L. Kuepfer, C. Becker, M. Block, K. Coboeken, T. Gaub, L. Goerlitz, J. Jaeger, R. Loosen, B. Ludewig, *et al.*, "A computational systems biology software platform for multiscale modeling and simulation: integrating whole-body physiology, disease biology, and molecular reaction networks," *Frontiers in physiology*, vol. 2, 2011.

[12] K. R. Rosen, "The history of medical simulation," *Journal of critical care*, vol. 23, no. 2, pp. 157–166, 2008.

[13] A. Cardoso, D. Osório, J. Leitão, V. Sousa, V. Graveto, and C. Teixeira, "Demonstration of modeling and simulation of physiological processes using a remote lab," in *Proceedings of the 3rd Experiment@ International Conference - exp.at'15*, 2015.

[14] A. Cardoso, D. Osório, J. Leitão, V. Sousa, and C. Teixeira, "A remote lab to simulate the physiological process of ingestion and excretion of a drug," *To be submitted to the International Journal of Online Engineering (iJOE)*, 2015.

[15] V. Sousa, "Platform for the supervision of remote systems using low cost devices," Master's thesis, FCTUC, 2015.

[16] S. S. Iyengar, ed., *Structuring Biological Systems: A Computer Modeling Approach*, ch. 5, p. 42. CRC Press, 1992.

[17] M. E. Wastney, B. H. Patterson, O. A. Linares, P. C. Greif, and R. C. Boston, *Investigating Biological Systems Using Modeling: Strategies and Software*, ch. 4, pp. 35–37. Academic Press, 1999.

[18] J. Semmlow, *Biomedical Engineering e-Mega Reference*, ch. 2.3, p. 67. Elsevier, 2009.

[19] A. C. Guyton, T. G. Coleman, and H. J. Granger, "Circulation: overall regulation," *Annual review of physiology*, vol. 34, no. 1, pp. 13–44, 1972.

[20] R. L. Hester, A. J. Brown, L. Husband, R. Iliescu, D. Pruett, R. Summers, and T. G. Coleman, "Hummod: a modeling environment for the simulation of integrative human physiology," *Frontiers in physiology*, vol. 2, 2011.

[21] D. Stefanovski, P. J. Moate, and R. C. Boston, "Winsaam: a windows-based compartmental modeling system," *Metabolism*, vol. 52, no. 9, pp. 1153–1166, 2003.

[22] C. Gille, C. Bölling, A. Hoppe, S. Bulik, S. Hoffmann, K. Hübner, A. Karlstädt, R. Ganeshan, M. König, K. Rother, *et al.*, "Hepatonet1: a comprehensive metabolic reconstruction of the human hepatocyte for the analysis of liver physiology," *Molecular systems biology*, vol. 6, no. 1, 2010.

[23] H. Dahari, J. E. Layden-Almer, E. Kallwitz, R. M. Ribeiro, S. J. Cotler, T. J. Layden, and A. S. Perelson, "A mathematical model of hepatitis c virus dynamics in patients with high baseline viral loads or advanced liver disease," *Gastroenterology*, vol. 136, no. 4, pp. 1402–1409, 2009.

[24] R. Banerjee, A. Das, U. C. Ghoshal, and M. Sinha, "Predicting mortality in patients with cirrhosis of liver with application of neural network technology," *Journal of gastroenterology and hepatology*, vol. 18, no. 9, pp. 1054–1060, 2003.

[25] F. Gorunescu, M. Gorunescu, E. El-Darzi, and S. Gorunescu, "An evolutionary computational approach to probabilistic neural network with application to hepatic cancer diagnosis," 2005.

[26] M. R. Mehta, C. Dasgupta, and G. R. Ullal, "A neural network model for kindling of focal epilepsy: basic mechanism," *Biological cybernetics*, vol. 68, no. 4, pp. 335–340, 1993.

[27] F. Wendling, J.-J. Bellanger, F. Bartolomei, and P. Chauvel, "Relevance of nonlinear lumped-parameter models in the analysis of depth-eeg epileptic signals," *Biological cybernetics*, vol. 83, no. 4, pp. 367–378, 2000.

[28] F. L. Da Silva, W. Blanes, S. N. Kalitzin, J. Parra, P. Suffczynski, and D. N. Velis, "Epilepsies as dynamical diseases of brain systems: basic models of the transition between normal and epileptic activity," *Epilepsia*, vol. 44, no. s12, pp. 72–83, 2003.

[29] G. Havenith, "Individualized model of human thermoregulation for the simulation of heat stress response," *Journal of Applied Physiology*, vol. 90, no. 5, pp. 1943–1954, 2001.

[30] M. Ursino, "Interaction between carotid baroregulation and the pulsating heart: a mathematical model," *American Journal of Physiology-Heart and Circulatory Physiology*, vol. 275, no. 5, pp. H1733–H1747, 1998.

[31] M. Ursino and C. A. Lodi, "Interaction among autoregulation, co2 reactivity, and intracranial pressure: a mathematical model," *American Journal of Physiology-Heart and Circulatory Physiology*, vol. 274, no. 5, pp. H1715–H1728, 1998.

[32] J. J. Batzel, F. Kappel, and S. Timischl-Teschl, "A cardiovascular-respiratory control system model including state delay with application to congestive heart failure in humans," *Journal of mathematical biology*, vol. 50, no. 3, pp. 293–335, 2005.

[33] C. Man, M. Camilleri, and C. Cobelli, "A system model of oral glucose absorption: validation on gold standard data," *Biomedical Engineering, IEEE Transactions on*, vol. 53, no. 12, pp. 2472–2478, 2006.

[34] A. R. Sedaghat, A. Sherman, and M. J. Quon, "A mathematical model of metabolic insulin signaling pathways," *American Journal of Physiology-Endocrinology and Metabolism*, vol. 283, no. 5, pp. E1084–E1101, 2002.

[35] G. Steil, A. Panteleon, and K. Rebrin, "Closed-loop insulin delivery - the path to physiological glucose control," *Advanced drug delivery reviews*, vol. 56, no. 2, pp. 125–144, 2004.

[36] R. Hovorka, V. Canonico, L. J. Chassin, U. Haueter, M. Massi-Benedetti, M. O. Federici, T. R. Pieber, H. C. Schaller, L. Schaupp, T. Vering, *et al.*, "Nonlinear model predictive control of glucose concentration in subjects with type 1 diabetes," *Physiological measurement*, vol. 25, no. 4, p. 905, 2004.

[37] G. Magombedze, P. Nduru, C. P. Bhunu, and S. Mushayabasa, "Mathematical modelling of immune regulation of type 1 diabetes," *Biosystems*, vol. 102, no. 2, pp. 88–98, 2010.

[38] M. König, S. Bulik, and H.-G. Holzhütter, "Quantifying the contribution of the liver to glucose homeostasis: a detailed kinetic model of human hepatic glucose metabolism," *PLoS computational biology*, vol. 8, no. 6, p. e1002577, 2012.

[39] R.-H. Lin, "An intelligent model for liver disease diagnosis," *Artificial Intelligence in Medicine*, vol. 47, no. 1, pp. 53–62, 2009.

[40] A. Onisko, M. J. Druzdzel, and H. Wasyluk, "A probabilistic causal model for diagnosis of liver disorders," in *Proceedings of the Seventh International Symposium on Intelligent Information Systems (IIS—98)*, p. 379, 1998.

[41] F. Gorunescu, S. Belciug, M. Gorunescu, and R. Badea, "Intelligent decision-making for liver fibrosis stadialization based on tandem feature selection and evolutionary-driven neural network," *Expert Systems with Applications*, vol. 39, no. 17, pp. 12824–12832, 2012.

[42] Y. Özbay, "A new method for diagnosis of cirrhosis disease: Complex-valued artificial neural network," *Journal of medical systems*, vol. 32, no. 5, pp. 369–377, 2008.

[43] Y.-W. Chen, J. Luo, C. Dong, X. Han, T. Tateyama, A. Furukawa, and S. Kanasaki, "Computer-aided diagnosis and quantification of cirrhotic livers based on morphological analysis and machine learning," *Computational and mathematical methods in medicine*, vol. 2013, 2013.

[44] X. Zhang, H. Fujita, M. Kanematsu, X. Zhou, T. Hara, H. Kato, R. Yokoyama, and H. Hoshi, "Improving the classification of cirrhotic liver by using texture features," in *Engineering in Medicine and Biology Society, 2005. IEEE-EMBS 2005. 27th Annual International Conference of the*, pp. 867–870, IEEE, 2006.

[45] T. Teorell, "Kinetics of distribution of substances administered to the body," *Arch Int Pharmacodyn Thé*, vol. 57, pp. 205–225, 1937.

[46] R. Bellman, J. A. Jacquez, and R. Kalaba, "Some mathematical aspects of chemotherapy. i. one-organ models.," *Bull. Math. Biophys.*, vol. 22, pp. 181–198, 1960.

[47] A. Dokoumetzidis, G. Valsami, and P. Macheras, "Modelling and simulation in drug absorption processes," *Xenobiotica*, vol. 37, no. 10-11, pp. 1052–1065, 2007.

[48] M. Di Muria, G. Lamberti, and G. Titomanlio, "Physiologically based pharmacokinetics: a simple, all purpose model," *Industrial & Engineering Chemistry Research*, vol. 49, no. 6, pp. 2969–2978, 2010.

[49] W. Huang, S. L. Lee, and X. Y. Lawrence, "Mechanistic approaches to predicting oral drug absorption," *The AAPS journal*, vol. 11, no. 2, pp. 217–224, 2009.

[50] C. C. Ko, B. M. Chen, J. Chen, Y. Zhuang, and K. C. Tan, "Development of a web-based laboratory for control experiments on a coupled tank apparatus," *Education, IEEE Transactions on*, vol. 44, no. 1, pp. 76–86, 2001.

[51] R. Dormido, H. Vargas, N. Duro, J. Sanchez, S. Dormido-Canto, G. Farias, F. Esquembre, and S. Dormido, "Development of a web-based control laboratory for automation technicians: The three-tank system," *Education, IEEE Transactions on*, vol. 51, no. 1, pp. 35–44, 2008.

[52] R. S. Schwartz, E. N. Brown, R. Lydic, and N. D. Schiff, "General anesthesia, sleep, and coma," *New England Journal of Medicine*, vol. 363, no. 27, pp. 2638–2650, 2010.

[53] C. Zaouter, M. Wehbe, S. Cyr, J. Morse, R. Taddei, P. A. Mathieu, and T. M. Hemmerling, "Use of a decision support system improves the management of hemodynamic and respiratory events in orthopedic patients under propofol sedation and spinal analgesia: a randomized trial," *Journal of clinical monitoring and computing*, vol. 28, no. 1, pp. 41–47, 2014.

[54] C. Rosow and P. J. Manberg, "Bispectral index monitoring," *Anesthesiology Clinics of North America*, vol. 19, no. 4, pp. 947–966, 2001.

[55] J. Liu, H. Singh, and P. F. White, "Electroencephalographic bispectral index correlates with intraoperative recall and depth of propofol-induced sedation," *Anesthesia & Analgesia*, vol. 84, no. 1, pp. 185–189, 1997.

[56] N. F. R. D. Lopes, "Monitorização cerebral inteligente durante a anestesia (monia)," Master's thesis, FCTUC, 2011.

[57] H. Kaul, N. Bharti, *et al.*, "Monitoring depth of anaesthesia," *Indian J Anaesth*, vol. 46, no. 4, pp. 323–332, 2002.

[58] M. F. O'Connor, S. M. Daves, A. Tung, R. I. Cook, R. Thisted, and J. Apfelbaum, "Bis monitoring to prevent awareness during general anesthesia," *Anesthesiology*, vol. 94, no. 3, pp. 520–2, 2001.

[59] M. S. Avidan, L. Zhang, B. A. Burnside, K. J. Finkel, A. C. Searleman, J. A. Selvidge, L. Saager, M. S. Turner, S. Rao, M. Bottros, *et al.*, "Anesthesia awareness and the bispectral index," *New England Journal of Medicine*, vol. 358, no. 11, pp. 1097–1108, 2008.

[60] M. T. Chan, B. C. Cheng, T. M. Lee, T. Gin, C. T. Group, *et al.*, "Bis-guided anesthesia decreases postoperative delirium and cognitive decline," *Journal of neurosurgical anesthesiology*, vol. 25, no. 1, pp. 33–42, 2013.

[61] R. Verma, A. K. Paswan, S. Prakash, S. K. Gupta, and P. Gupta, "Sedation with propofol during combined spinal epidural anesthesia: Comparison of dose requirement of propofol with and without bis monitoring," *Anaesthesia, Pain & Intensive Care*, vol. 17, no. 1, pp. 14–17, 2013.

[62] A. E. Ibrahim, J. K. Taraday, E. D. Kharasch, *et al.*, "Bispectral index monitoring during sedation with sevoflurane, midazolam, and propofol," *Anesthesiology*, vol. 95, no. 5, pp. 1151–1159, 2001.

[63] M. Doi, R. Gajraj, H. Mantzaridis, and G. Kenny, "Relationship between calculated blood concentration of propofol and electrophysiological variables during emergence from anaesthesia: comparison of bispectral index, spectral edge frequency, median frequency and auditory evoked potential index.," *British Journal of Anaesthesia*, vol. 78, no. 2, pp. 180–184, 1997.

[64] R. R. Riker, G. L. Fraser, L. E. Simmons, and M. L. Wilkins, "Validating the sedation-agitation scale with the bispectral index and visual analog scale in adult icu patients after cardiac surgery," *Intensive care medicine*, vol. 27, no. 5, pp. 853–858, 2001.

[65] M. Jamei, D. Turner, J. Yang, S. Neuhoff, S. Polak, A. Rostami-Hodjegan, and G. Tucker, "Population-based mechanistic prediction of oral drug absorption," *The AAPS journal*, vol. 11, no. 2, pp. 225–237, 2009.

[66] Y. Kwon, ed., *Handbook of Essential Pharmacokinetics, Pharmacodynamics and Drug Metabolism for Industrial Scientists*, ch. 5 - Distribution and 6 - Clearance, pp. 73, 83. Springer Science and Business Media, 2001.

[67] J. Fan and I. A. de Lannoy, "Pharmacokinetics," *Biochemical Pharmacology*, vol. 87, no. 1, pp. 93–120, 2014.

[68] L. Prescott, "Kinetics and metabolism of paracetamol and phenacetin.," *British journal of clinical pharmacology*, vol. 10, no. S2, pp. 291S–298S, 1980.

[69] R. L. Daugherty, J. B. Franzini, and E. J. Finnemore, *Fluid Mechanics with Engineering Applications*, p. 467. McGraw-Hill, Inc., 8 ed., 1985.

[70] V. L. Streeter, E. B. Wylie, and K. W. Bedford, *Fluid Mechanics*, p. 1985. McGraw-Hill, Inc., 9 ed., 1998.

[71] R. Rhoades and D. R. Bell, eds., *Medical Physiology: Principles for Clinical Medicine*, ch. 6 - Renal physiology and body fluids, p. 440. Lippincott Williams and Wilkins, 2009.

[72] B. G. Liptak, *Instrument Engineers' Handbook, Fourth Edition, Volume Two: Process Control and Optimization*, vol. 2, ch. 2.2, p. 116. CRC Press, fourth ed., 2005.

[73] E. Alexopoulos, "Introduction to multivariate regression analysis," *Hippokratia*, vol. 14, no. Suppl 1, p. 23, 2010.

[74] B. Hidalgo and M. Goodman, "Multivariate or multivariable regression?," *American journal of public health*, vol. 103, no. 1, pp. 39–40, 2013.

[75] Health Quality Ontario, "Bispectral index monitor: an evidence-based analysis.," *Ontario health technology assessment series*, vol. 4, pp. 1–70, Jun 2004.

[76] A. Ekman, M.-L. Lindholm, C. Lennmarken, and R. Sandin, "Reduction in the incidence of awareness using bis monitoring," *Acta Anaesthesiologica Scandinavica*, vol. 48, no. 1, pp. 20–26, 2004.

Appendix A

State of the art appendix

VARIABLES		Physically System	General Description	Electrical	Hydraulical	Pneumatical	Thermal	Translational	Rotational
	PRIMARY	Transversal Variable e(t)	Voltage, Pressure Velocity	U(t); Voltage	P(t); Pressure	P(t); Pressure	T(t); Temperature	V(t); Velocity	$\omega(t)$; Angular Velocity
		Transit Variable f(t)	Current, Flow Force, Momentum	i(t); Current	$\dot{V}(t)$; Volume Flow	$\dot{m}(t)$; Mass Flow	$\dot{q}(t)$; Heat Flow	f(t); Force	M(t); Torque
		e(t) Product	Power supplied to the element	$p(t)=u(t)\cdot i(t)$	$p(t)=P(t)\cdot\dot{V}(t)$	$p(t)=P(t)\cdot\dot{m}(t)$	$p(t)=\dot{q}(t)$	$p(t)=V(t)\cdot f(t)$	$p(t)=\omega(t)xM(t)$
		e(t) Relation	Power Consumption $e(t)=R\cdot f(t)$	R; Electrical Resistance	$R=\frac{8 l \eta}{\pi r^4}$ Flow - resistance	identical to hydraulical	Thermal Resistance $R_F=\frac{1}{\lambda A}$ (Flow) $R_T=\frac{1}{\alpha A}$ (Transm.) $R_C=\frac{1}{mc}$ (Convect.)	d^{-1}; Damping - factor	d_φ^{-1}; Damping-factor
	INTEGRAL	$\int e(t)\,dt$	$F(t)=1/L\cdot\int e(t)\,dt$	L; Inductor	$\frac{\rho l}{\pi r^2}$; Inertance	$\frac{\rho l}{\pi r^2}$; Inertance	———	c^{-1}; Spring - constant	c_φ^{-1}; Spring - constant
		$\int f(t)\,dt$	$e(t)=1/C\cdot\int f(t)\,dt$	C; Capacitor	$\frac{A}{\rho g}$; Hydraulic Capacity	$\frac{m_o}{\delta_o}=\frac{V}{R\cdot T}$; Pneumatic Capacity	m • c; Thermal Capacity	M; Mass	Θ; Moving Mass
		$\int e(t)\,f(t)\,dt$	Energy done on system	E_M:Magnetic Energy of inductor E_E:Electric Energy of capacitor	E_K:Kinetic Energy of fluid flow E_P:Potential Energy of pressure head	E_K:Kinetic Energy of pneumatic flow E_P:Potential Energy of pressure	E_P:Thermal Potential Energy of stored heat	E_K:Kinetic Energy of moving mass E_P:Potential Energy of compressed Spring	E_K:Kinetic Energy of rotating mass E_P:Potential Energie of twisted spring
		Symbols		R L C	C	C	T_1 R T_2 $\dot{q}$ T_1 C T_2	R L M C	L M C

Figure A.1: Table of correspondence to build equivalent models. (Taken from [2])

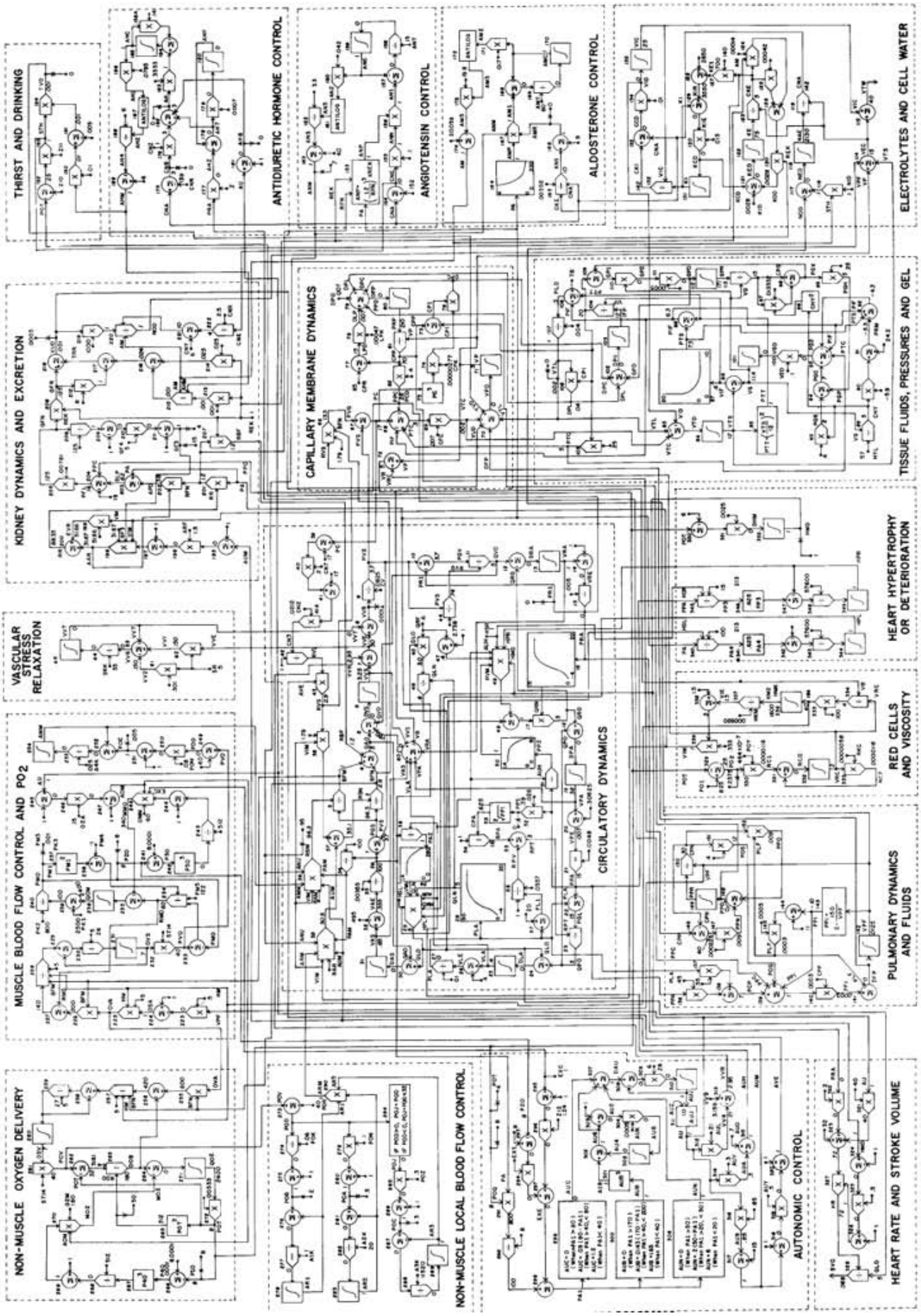

Figure A.2: Arthur Guyton's computer model of the cardiovascular system. Retrieved October 6, 2015, from `http://ajpregu.physiology.org/content/287/5/R1009`

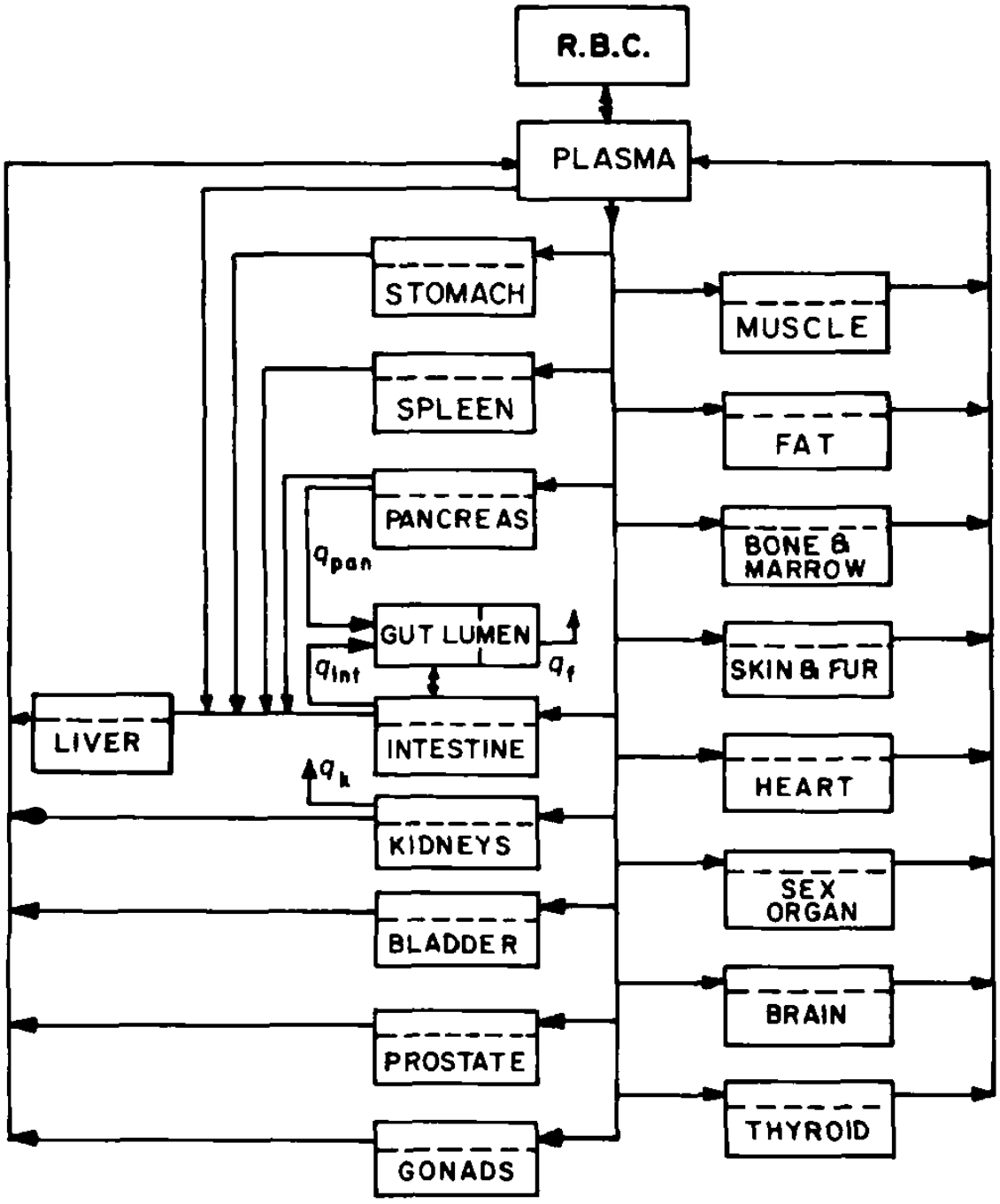

Figure A.3: Example of a physiologically based pharmacokinetic model flow scheme. (Taken from [8])

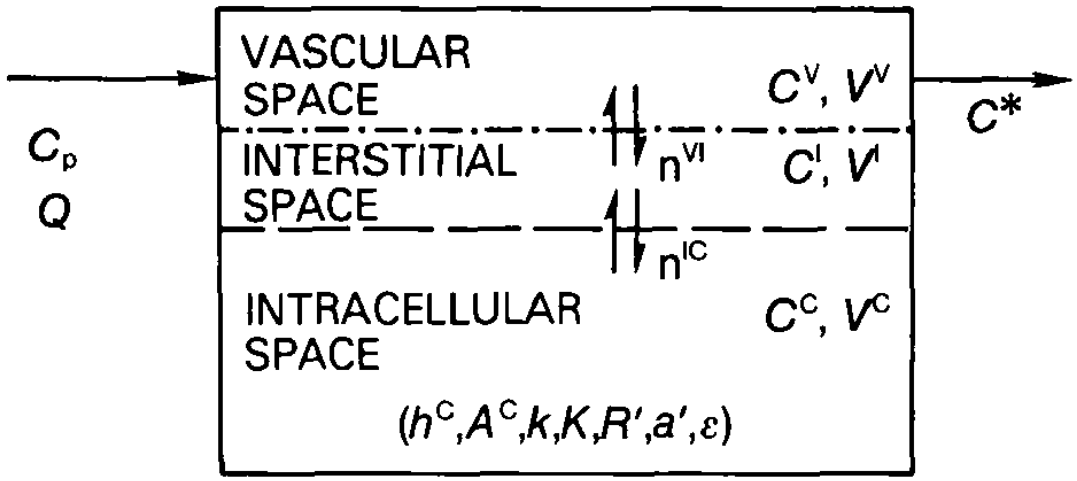

Figure A.4: Representation of the vascular, interstitial and intracellular spaces of an organ. The flux of the substance occurs across the dashed lines; the arrows represent the direction of the blood flow. (Taken from [8])

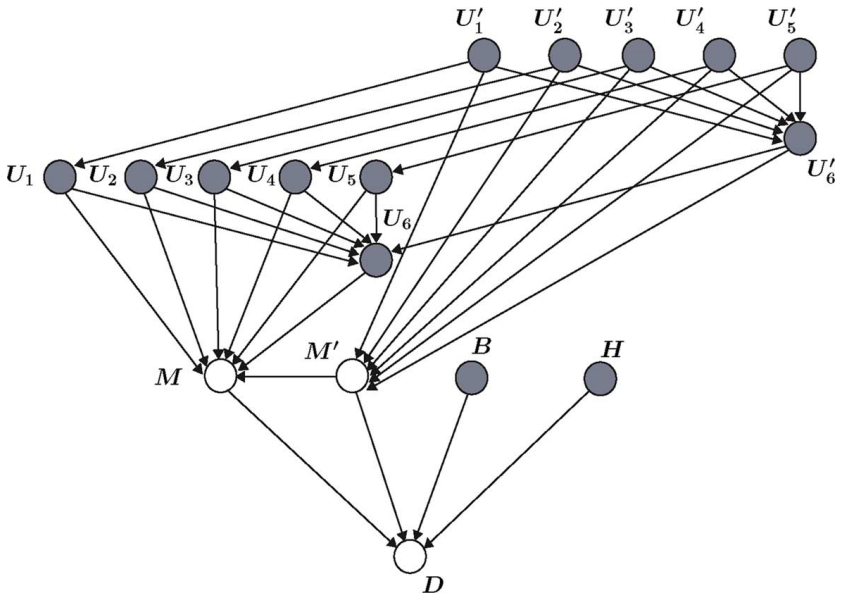

Figure A.5: Graph of a Bayesian network capturing the relationship between the MAAS current (M) and previous score (M') and other observable factors; namely, current and previous objective assessments of facial expression U_1, U'_1, gross motor movement U_2, U'_2, guarding U_3, U'_3, heart rate and blood pressure stability U_4, U'_4, non-cardiac sympathetic stability U_5, U'_5, non-verbal pain scale U_6, U'_6, blood pressure (B), heart rate H, and required drug dose D. (Taken from [9])

Appendix B

Centre tank flow coefficient determination

In order to find C, ten discharges were made. An example of one of the discharges is shown in Figure B.1.(a).(a). As mentioned, the valve was open at 25%.

The data acquired is expressed in Volts. To convert from a voltage to a water level, a simple linear regression was performed using the initial level and final level with the first and last voltage values.

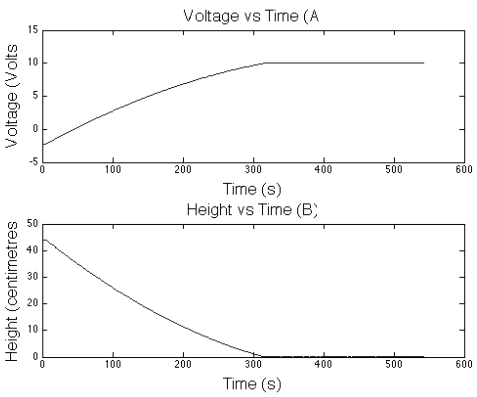

(a) Raw data in Volts (a) and the conversion to centimetres (b).

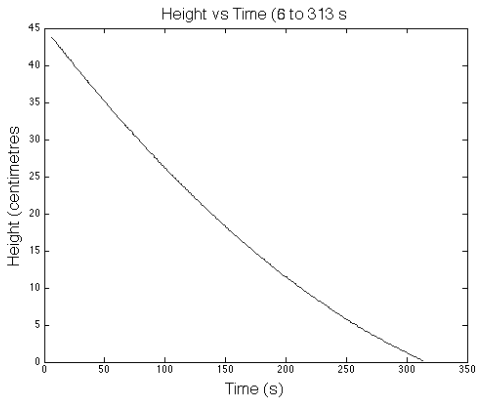

(b) Region used to determine C.

Figure B.1: Analog equivalent models of physiological systems.

The initial water level value for each of the 10 discharges are shown in Table B.1.

From the level versus time curve (Figure B.1.(a).(b)), a linear region was chosen in order to find the value of C.

This region is found automatically by selecting all the values higher than 2 millimetres and the lower than the maximum minus 2 millimetres.

The 2 millimetres margins were added in order to reduce the bottom instability introduced by the output valve and to cut the values corresponding to the time it took between starting the measurements and opening the valve.

Since equation 3.9 is a differential equation, a numerical integration method is required to solve it. In this case, Euler's method is enough, since the process in study has a slow rate of change.

Table B.1: Values for the flow coefficient and initial heights from ten centre tank discharges with valve$_{OutCT}$ at 25% opening.

Centre Tank

Initial Height (cm)	Flow Coefficient
47.0	0.1607
43.0	0.2097
44.1	0.2518
43.5	0.2052
44.5	0.1560
43.5	0.1452
41.0	0.1421
43.0	0.1900
42.0	0.1577
42.0	0.2257

ΔT = 0.6833 (s)
ΔC = 0.1844

$$H(n+1) = H(n) + \Delta H(n) \times \Delta t \tag{B.1}$$

In equation B.1, n represents the discrete time variable and Δt the time delta between each pair of samples. Replacing equation 3.9 in B.1:

$$H(n+1) = H(n) + \frac{Q_{in}(n) - aC\sqrt{2gH(n)}}{A} \times \Delta t \tag{B.2}$$

And finally resolving equation B.2 in order of the flow coefficient C and assuming that $Q_{in} = 0$:

$$C(n) = -\frac{(H(n+1) - H(n))A}{\Delta t \times a\sqrt{2gH(n)}} \tag{B.3}$$

Table B.2 provides the values used for the remaining constants.

Table B.2: Constants to be used in equation (B.3).

Parameter	**Description**	**Value**
a	Cross section area of the discharge pipe	0.5 cm^2
A	Cross section area of the tank	154 cm^2
g	Gravitational Acceleration	980.665 $\frac{cm}{s^2}$

Since there are some spikes in the signal, a region between 0.68 and 0.72 seconds for the time deltas was chosen.

Using the values selected within the time delta value region, the flow and flow coefficient were calculated.

In Figure B.3 in the flow coefficient plot, 2 different values are shown for the mean. From around 200 seconds, there is a increase in the flow coefficient. This phenomena

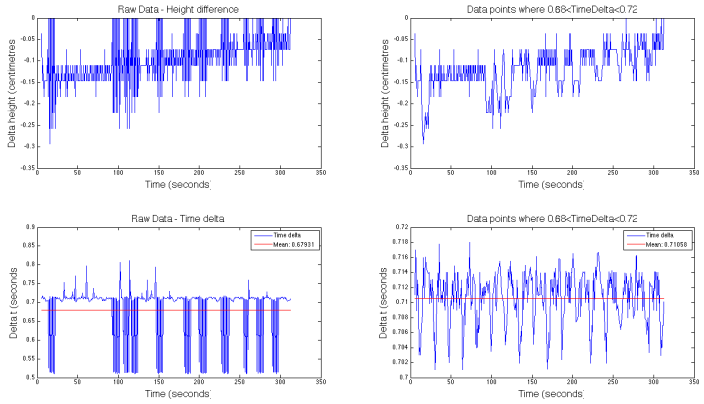

Figure B.2: Before and after spike removal in the time deltas and height difference data.

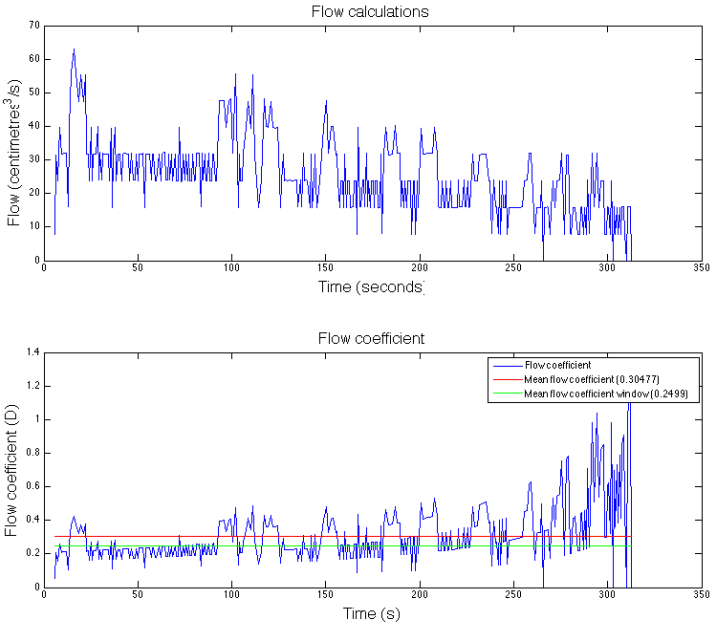

Figure B.3: Flow and flow coefficient representation.

could be the result of the perturbations to the flow introduced by the valve at low water levels. This flow coefficient increase causes a subsequent increase in the coefficient mean.

The second mean (green line) was calculated using only the values for the flow coefficient that were below 200 seconds.

In Table B.3, the mean value for all runs are presented, as well as the final flow coefficient value.

Figure B.4 is the comparison between two simulations using a different flow coefficient and the raw data.

Table B.3: Flow coefficient for a valve 25% opened.

Flow coefficient
0.1426
0.2112
0.2499
0.2036
0.1578
0.1463
0.1350
0.1899
0.1564
0.2218
$\Delta C = 0.1814$

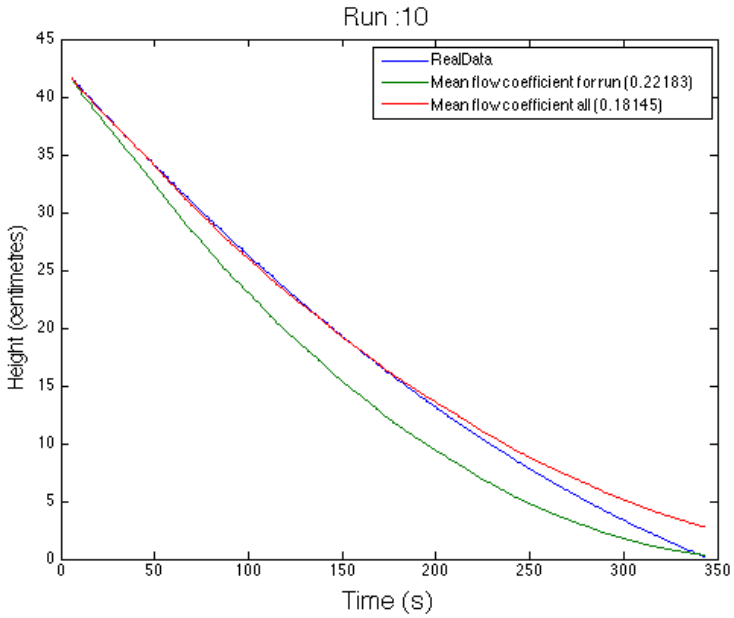

Figure B.4: Simulation using run 10 mean and the final value for the flow coefficient.

The same experiment/procedure was applied to determine the flow coefficients of the valve connecting the left and centre tank and the outflow valve in the right tank.

The flow coefficients used in this work are presented in Table B.4.

Table B.4: Flow coefficient used in this work.

C_{LC}	C_{outCT}	C_{outRT}
0.4180	0.1814	0.6619

Appendix C

Web-based simulation

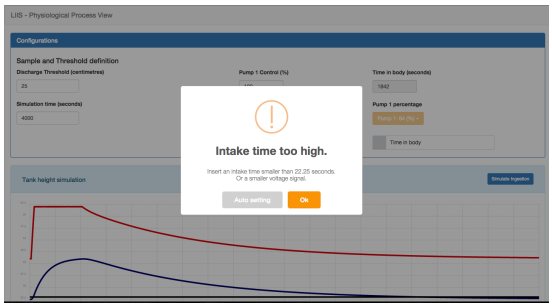

(a) Screenshot of the generated warning.

(b) Screenshot after simulating a saturated ingestion.

Figure C.1: Screenshots of the online simulation platform during a warning and a saturated simulation.

Table C.1: Fitting coefficients for the maximum intake without saturation of the left tank.

Fitted equation:
$t = p_1 \times u^7 + p_2 \times u^6 + p_3 \times u^5 + p_4 \times u^4 + p_5 \times u^3 + p_6 \times u^2 + p_7 \times u + p_8$

Coefficients	Values
p_1	-1.9698
p_2	50.7943
p_3	-557.4949
p_4	3379.3
p_5	-12237
p_6	26539
p_7	-32066
p_8	16841

Table C.2: Fitting coefficients and time intervals of each of first pump time in blood stream to intake time mapping.

Fitted equation:
$t_{Intake} = p_1 \times t^3_{Bloodstream} + p_2 \times t^2_{Bloodstream} + p_3 \times t_{Bloodstream} + p_4$

Pump %	Lower Interval (seconds)	Higher Interval (seconds)	p_1	p_2	p_3	p_4
40	622	2813	10.4×10^{-9}	-1.94×10^{-5}	3.82×10^{-2}	10.53
42	752	2762	9.64×10^{-9}	-1.95×10^{-5}	3.73×10^{-2}	8.07
44	866	2717	9.03×10^{-9}	-1.96×10^{-5}	3.75×10^{-2}	6.03
46	957	2680	8.49×10^{-9}	-1.95×10^{-5}	3.71×10^{-2}	4.42
48	1058	2646	7.91×10^{-9}	-1.87×10^{-5}	3.56×10^{-2}	3.71
50	1141	2618	7.37×10^{-9}	-1.78×10^{-5}	3.39×10^{-2}	3.40
52	1216	2598	7.01×10^{-9}	-1.75×10^{-5}	3.32×10^{-2}	2.69
54	1286	2575	6.38×10^{-9}	-1.55×10^{-5}	2.95×10^{-2}	3.98
56	1351	2558	6.07×10^{-9}	-1.50×10^{-5}	2.85×10^{-2}	3.85
58	1412	2544	6.21×10^{-9}	-1.69×10^{-5}	3.21×10^{-2}	0.90
60	1469	2528	5.96×10^{-9}	-1.66×10^{-5}	3.15×10^{-2}	0.62
62	1522	2516	5.76×10^{-9}	-1.64×10^{-5}	3.12×10^{-2}	0.13
64	1573	2508	5.58×10^{-9}	-1.63×10^{-5}	3.10×10^{-2}	-0.30
66	1621	2498	5.41×10^{-9}	-1.61×10^{-5}	3.08×10^{-2}	-0.65
68	1667	2489	5.24×10^{-9}	-1.58×10^{-5}	3.03×10^{-2}	-0.85
70	1710	2483	6.57×10^{-9}	-2.47×10^{-5}	4.84×10^{-2}	-13.45
72	1751	2472	4.93×10^{-9}	-1.53×10^{-5}	2.99×10^{-2}	-1.11
74	1791	2465	4.80×10^{-9}	-1.51×10^{-5}	2.92×10^{-2}	-1.35
76	1829	2465	4.39×10^{-9}	-4.46×10^{-5}	9.08×10^{-2}	-44.38
78	1866	2457	4.56×10^{-9}	-1.47×10^{-5}	2.86×10^{-2}	-1.59
80	1901	2450	4.57×10^{-9}	-1.54×10^{-5}	3.00×10^{-2}	-2.91
82	1935	2445	4.32×10^{-9}	-1.42×10^{-5}	2.77×10^{-2}	-1.57
84	1968	2444	13.8×10^{-9}	-7.63×10^{-5}	16.2×10^{-2}	-48.23
86	1999	2435	4.45×10^{-9}	-1.60×10^{-5}	3.18×10^{-2}	-5.15
88	2030	2431	4.07×10^{-9}	-1.39×10^{-5}	2.74×10^{-2}	-2.20
90	2059	2429	4.29×10^{-9}	-1.58×10^{-5}	3.15×10^{-2}	-5.40
92	2088	2425	3.75×10^{-9}	-1.25×10^{-5}	2.43×10^{-2}	-0.29
94	2116	2426	8.31×10^{-9}	-54.6×10^{-5}	1.22	-891.40
96	2143	2422	9.29×10^{-9}	-61.6×10^{-5}	1.38	-1021.00
98	2169	2419	4.67×10^{-9}	-30.6×10^{-5}	68.8×10^{-2}	-502.20
100	2195	2415	1.92×10^{-9}	-0.13×10^{-5}	-0.11×10^{-2}	18.25

Appendix D

Drug effect and cause

Fentanyl

Effect: Fentanyl is an opioid medication.
Usages: Fentanyl is used as part of anaesthesia to help prevent pain after surgery or other medical procedure.

Droperidol

Effect: Reducing nausea and vomiting during surgeries and diagnostic procedures.
Usages: Droperidol is a tranquilizer. It is unknown exactly how droperidol works.

Thiopental

Effect: It works by depressing the central nervous system, causing mild sedation or sleep.
Usages: Thiopental is a barbiturate. Causing drowsiness or sleep before surgery or certain medical procedures. It is also used to stop seizures.

Cisatracurium

Effect: It works by blocking the effects of acetylcholine, a chemical involved in muscle contraction. This relaxes muscles in the body before surgery or insertion of a breathing tube.
Usages: Cisatracurium is a non depolarizing skeletal muscle relaxant. Providing muscle relaxation during surgery, medically assisted breathing, or easier insertion of a breathing tube.

Sevoflurane

Effect: It works by depressing activity in the central nervous system, which causes loss of consciousness.
Usages: Sevoflurane is an anesthetic. Causing general anesthesia (loss of consciousness) before and during surgery.

Atropine

Effect: Atropine produces many effects in the body.

Usages: It is used during surgery to maintain proper heart function; during emergencies involving the heart; and to treat certain heart disorders.

Rocuronium

Effect: Rocuronium is used to relax the muscles. It works by blocking the signals between the nerves and the muscles.

Usages: Rocuronium is given before general anesthesia in preparing for surgery. Rocuronium helps to keep the body still during surgery. It also relaxes the throat so a breathing tube can be more easily inserted before the surgery.

Ondansetron

Effect: Ondansetron blocks the actions of chemicals in the body that can trigger nausea and vomiting.

Usages: Ondansetron is used to prevent nausea and vomiting that may be caused by surgery.

Ketorolac

Effect: Ketorolac is an NSAID. Exactly how it works is not known. It may block certain substances in the body that are linked to inflammation. NSAIDs treat the symptoms of pain and inflammation.

Usages: The short-term (up to 5 days) treatment of moderately severe pain (usually after surgery).

Methylprednisolone

Effect: Methylprednisolone is a steroid that prevents the release of substances in the body that cause inflammation.

Usages: Methylprednisolone is used to treat many different inflammatory.

Propofol

Effect: Propofol (Diprivan) slows the activity of the brain and nervous system.

Usages: Propofol is used to help relax before and during general anaesthesia for surgery or other medical procedures. It is also used in critically ill patients who require a breathing tube connected to a ventilator (a machine that moves air in and out of the lungs when a person cannot breathe on their own).

Appendix E

Dataset and drug relation

Patient three: Fentanyl, droperidol, thiopental, cisatracurium, sevoflurane and atropine.

Patient four: Fentanyl, droperidol, propofol, cisatracurium, sevoflurane and atropine.

Patient five: Fentanyl, droperidol, rocuronium, sevoflurane and atropine.

Patient seven: Fentanyl, droperidol, propofol, cisatracurium, atropine, ondansetron, ketorolac and methylprednisolone.

Patient ten: Fentanyl, propofol, sevoflurano and atropine.

Appendix F

Correlation between the BIS with the rest of the variables for each dataset - Full duration and by intervals

For each following table, the green colour represents correlated values, while red represents uncorrelated values. For a variables to be considered correlated, the correlation value has to be higher than 50%.

Table F.1: Correlation between the BIS and patient three dataset.

Variable	Full duration	Conscience falling	Anaesthesia	Conscience rising
HR	0	0	0	1
SpO_2	1	1	0	0
PLS	0	0	0	1
$etCO_2$	1	1	0	0
iCO_2	0	0	0	0
RRc	1	1	0	1
PIP	0	0	0	0
PEEP	1	0	0	0
MAP	1	1	0	0
MVe	1	1	0	1
TVe	1	1	0	0
RRv	1	1	0	0
NBPS	0	1	0	0
NBPD	0	0	0	0
NBPM	0	1	0	0
iO_2	0	0	0	0
etO_2	0	0	0	0
etSEV	1	1	0	0
iSEV	1	1	0	0
etN_2O	0	0	0	0
iN_2O	0	0	0	0

Table F.2: Correlation between the BIS and patient four dataset.

Variable	Full duration	Conscience falling	Anaesthesia	Conscience rising
HR	1	1	0	1
SpO_2	0	0	0	0
PLS	1	1	0	1
$etCO_2$	1	1	1	0
iCO_2	0	0	0	1
RRc	0	0	0	1
PIP	1	1	0	0
PEEP	1	1	0	0
MAP	1	1	0	0
MVe	1	1	0	0
TVe	1	1	0	0
RRv	1	0	0	1
NBPS	0	0	0	1
NBPD	0	0	0	1
NBPM	0	0	0	1
iO_2	0	0	0	1
etO_2	0	0	0	1
etSEV	1	0	0	1
iSEV	1	0	0	1
etN_2O	0	0	1	1
iN_2O	0	0	1	1

Table F.3: Correlation between the BIS and patient five dataset.

Variable	Full duration	Conscience falling	Anaesthesia	Conscience rising
HR	0	0	0	1
SpO_2	1	0	0	1
PLS	0	0	0	1
$etCO_2$	1	0	0	1
iCO_2	0	0	0	0
RRc	1	0	0	1
PIP	1	1	0	1
PEEP	1	1	0	1
MAP	1	1	0	1
MVe	1	1	0	1
TVe	1	0	0	1
RRv	1	0	0	1
NBPS	0	0	0	1
NBPD	0	0	0	1
NBPM	0	0	0	1
iO_2	1	0	0	1
etO_2	1	0	0	1
etSEV	1	0	0	1
iSEV	1	0	0	1
etN_2O	0	0	0	0
iN_2O	0	0	0	0

Table F.4: Correlation between the BIS and patient seven dataset.

Variable	Full duration	Conscience falling	Anaesthesia	Conscience rising
HR	0	1	0	0
SpO_2	0	0	0	0
PLS	0	1	0	0
$etCO_2$	1	0	0	1
iCO_2	0	0	0	0
RRc	1	0	0	0
PIP	1	0	0	0
PEEP	0	0	0	1
MAP	1	0	1	0
MVe	1	0	1	1
TVe	&1	0	1	0
RRv	0	0	0	0
NBPS	0	1	0	0
NBPD	0	0	0	0
NBPM	0	0	0	0
iO_2	1	1	1	1
etO_2	1	0	1	0
etSEV	1	0	1	1
iSEV	1	0	1	1
etN_2O	0	0	0	0
iN_2O	0	0	0	0

Table F.5: Correlation between the BIS and patient nine dataset.

Variable	**Full**
HR	1
SpO_2	0
PLS	1
$etCO_2$	0
iCO_2	0
RRc	1
PIP	1
PEEP	1
MAP	1
MVe	1
TVe	1
RRv	0
NBPS	1
NBPD	0
NBPM	0
iO_2	1
etO_2	1
etSEV	0
iSEV	0
etN_2O	0
iN_2O	0

Table F.6: Correlation between the BIS and patient nine dataset.

Variable	**Full**
HR	0
SpO_2	0
PLS	0
$etCO_2$	0
iCO_2	0
RRc	1
PIP	0
PEEP	1
MAP	0
MVe	1
TVe	1
RRv	1
NBPS	0
NBPD	0
NBPM	0
iO_2	1
etO_2	0
etSEV	0
iSEV	0
etN_2O	0
iN_2O	0

Table F.7: Correlation between the BIS and patient ten dataset.

Variable	Full duration	Conscience falling	Anaesthesia	Conscience rising
HR	0	0	0	0
SpO_2	0	0	0	1
PLS	0	0	0	0
etCO_2	1	0	0	1
iCO_2	0	0	0	0
RRc	1	0	0	0
PIP	1	1	0	1
PEEP	1	0	0	0
MAP	0	1	0	0
MVe	1	0	0	0
TVe	1	0	0	1
RRv	0	0	0	0
NBPS	1	0	0	1
NBPD	0	0	0	1
NBPM	1	1	0	1
iO_2	1	0	0	1
etO_2	1	0	0	1
etSEV	1	0	1	1
iSEV	1	0	1	1
etN_2O	0	0	0	0
iN_2O	0	0	0	0

Appendix G

Correlation tables between each BIS correlated variable and the others - For each interval

For each following table, the green colour represents correlated values, while red represents uncorrelated values.
For a variables to be considered correlated, the correlation value has to be higher than 50%.

Table G.1: Correlation between each BIS correlated variable and the other, for the full duration of the surgery.

	$etCO_2$	RRc	PIP	PEEP	MAP	MVe	TVe	RRv	iO_2	etO_2	etSEV	iSEV
$etCO_2$		0.7676	0.5254	0.6846	0.6220	0.6831	0.5286	0.5286	-0.3165	-0.2585	0.6818	0.5935
RRc	0.7676		0.5857	0.7847	0.7543	0.8858	0.8313	0.6047	-0.4513	-0.2585	0.6818	0.6688
PIP	0.5254	0.5857		0.7022	0.8513	0.7189	0.7303	0.4922	-0.2728	-0.3230	0.5314	0.5187
PEEP	0.6846	0.7847	0.7022		0.8137	0.8222	0.8305	0.4793	-0.3941	-0.4644	0.6387	0.6276
MAP	0.6220	0.7543	0.8513	0.8137		0.9020	0.9069	0.4444	-0.4695	-0.5088	0.7314	0.7108
MVe	0.6831	0.8858	0.7189	0.8222	0.9020		0.9585	0.5415	-0.5503	-0.5945	0.7839	0.7600
TVe	0.6600	0.8313	0.7303	0.8305	0.9069	0.9585		0.4305	-0.5764	-0.6154	0.8096	0.7938
RRv	0.5286	0.6047	0.4922	0.4793	0.4444	0.5415	0.4305		-0.1329	-0.2296	0.3221	0.3011
iO_2	-0.3165	-0.4513	-0.2728	-0.3941	-0.4695	-0.5503	-0.5764	-0.1329		0.8148	-0.6346	-0.6313
etO_2	-0.2585	-0.5391	-0.3230	-0.4644	-0.5088	-0.5945	-0.6154	-0.2296	0.8148		-0.7167	-0.6858
etSEV	0.6818	0.7132	0.5314	0.6387	0.7314	0.7839	0.8096	0.3221	-0.6346	-0.7167		0.9851
iSEV	0.5935	0.6688	0.5187	0.6276	0.7108	0.7600	0.7938	0.3011	-0.6313	-0.6858	0.9851	

Table G.2: Correlation between each BIS correlated variable and the other, for the conscience falling phase of the surgery.

	PIP	PEEP	MAP	MVe	TVe
PIP		0.4098	0.5081	0.3144	0.2590
PEEP	0.4098		0.7057	0.6620	0.6410
MAP	0.5081	0.7057		0.8826	0.7802
MVe	0.3144	0.6620	0.8826		0.8954
TVe	0.2590	0.6410	0.7802	0.8954	

Table G.3: Correlation between each BIS correlated variable and the other, for the anaesthesia falling phase of the surgery.

	etSEV	iSEV
etSEV		0.9491
iSEV	0.9491	

Table G.4: Correlation between each BIS correlated variable and the other, for the waking phase of the surgery.

	HR	SpO_2	PLS	$etCO_2$	RRc	PIP	PEEP	MVe	TVe	RRv	iO_2	etO_2	etSEV	iSEV
HR		0.1531	0.9669	0.3506	0.2881	-0.5286	-0.1277	-0.4119	-0.2692	-0.1652	0.0806	-0.1740	-0.2528	-0.2193
SpO_2	0.1531		0.0719	-0.2928	-0.0315	-0.2096	-0.0522	0.0769	0.1211	-0.0780	0.3458	0.4328	-0.3534	-0.3529
PLS	0.9669	0.0719		0.3314	0.3068	-0.5556	-0.0680	-0.3048	-0.2295	-0.1530	0.0291	-0.1084	-0.3184	-0.2904
$etCO_2$	0.3506	-0.2928	0.3314		0.6205	-0.1616	0.0485	-0.1364	0.0423	0.1704	-0.0436	-0.7128	0.1568	0.1184
RRc	0.2881	-0.0315	0.3068	0.6205		-0.1512	0.2948	0.1805	0.2656	0.2120	-0.1285	-0.2604	-0.1493	-0.1789
PIP	-0.5286	-0.2096	-0.5556	-0.1616	-0.1512		0.0171	0.4306	0.1341	0.1618	-0.2370	0.1448	0.4068	0.3943
PEEP	-0.1277	-0.0522	-0.0680	0.0485	0.2948	0.0171		0.5911	0.1721	0.3824	-0.2532	0.1447	0.0360	0.0150
MVe	-0.4119	0.0769	-0.3048	-0.1364	0.1805	0.4306	0.5911		0.5073	0.2049	-0.0898	0.3856	-0.1668	-0.2005
TVe	-0.2692	0.1211	-0.2295	0.0423	0.2656	0.1341	0.1721	0.5073		-0.2935	-0.2147	0.0502	-0.2148	-0.2498
RRv	-0.1652	-0.0780	-0.1530	0.1704	0.2120	0.1618	0.3824	0.2049	-0.2935		0.1989	0.0954	0.2031	0.1757
iO_2	0.0806	0.3458	0.0291	-0.0436	-0.1285	-0.2370	-0.2532	-0.0898	-0.2147	0.1989		0.2985	-0.2686	-0.2808
etO_2	-0.1740	0.4328	-0.1084	-0.7128	-0.2604	0.1448	0.1447	0.3856	0.0502	0.0954	0.2985		-0.4504	-0.4448
etSEV	-0.2528	-0.3534	-0.3184	0.1568	-0.1493	0.4068	0.0360	-0.1668	-0.2148	0.2031	-0.2686	-0.4504		0.9902
iSEV	-0.2193	-0.3529	-0.2904	0.1184	-0.1789	0.3943	0.0150	-0.2005	-0.2498	0.1757	-0.2808	-0.4448	0.9902	

Appendix H

Paper submitted to exp.at'15 conference

Demonstration of modeling and simulation of physiological processes using a remote lab

Alberto Cardoso, Daniel Osório, Joaquim Leitão, Vitor Sousa, Vitor Graveto, César Teixeira
Centre for Informatics and Systems of the University of Coimbra (CISUC)
Department of Informatics Engineering, University of Coimbra
Coimbra, Portugal
alberto@dei.uc.pt, daniel.osorio@student.fisica.uc.pt, {jpleitao, vhsousa, vgraveto}@student.dei.uc.pt, cteixei@dei.uc.pt

***Abstract*—Remote and virtual labs represent a very important support in engineering teaching and can be used to improve the students learning process, for example of Biomedical Engineering courses, on topics such as the identification of models and control systems. This paper describes the demonstration of an online experiment, supported by a three-tank lab system, to model, simulate and monitoring a physiological process as the system of ingestion and excretion of a drug. A Web platform is used to interact with the remote and virtual lab, where students can visualize and obtain data in real time from the remote system.**

Keywords—Online experimentation; remote and virtual labs; physiological processes; biomedical engineering

I. INTRODUCTION

The understanding of physiological processes and their dynamics can represent a difficulty for students, which can be overcome by considering computer-based learning approaches with the support of online experimentation. Mathematical models have proven to be a valuable tool for the analysis and synthesis of physiological processes [1]. The use of experimental modules to represent its structure and function can contribute significantly to understand it and improve the learning process.

Some physiological systems can be divided into subsystems and modelled by compartment models to represent the dynamics of the overall system. In this context, a laboratory system as the three-tank process has the necessary characteristics to be a simplified representation of, for example, a system of ingestion and excretion of a drug.

The development of remote and virtual labs can represent a valuable support for student's learning, enabling a wide access to the experiments and allowing the interaction in real time with the lab system to perform practical experiences, visualising and analysing the dynamic behaviour of the system [2]. Experiential learning focuses on individual learning plays a central role within science and technology curriculum at all levels of higher education [3]. Similarly to traditional laboratories, remote labs provide students with particular engineering experience and allow them to explore the systems and their real behaviours.

Systems analysis systems is a very important topic in biomedical engineering because it is the basis to model, simulate and control different physiological processes [4].

This paper pretends to present the demonstration of an online experiment, designed to be accomplished in courses about computational models of physiological processes and algorithms for diagnosis and self-regulation of a Master Degree on Biomedical Engineering, in a blended learning context.

II. THE PHYSIOLOGICAL PROCESS

This work considers the modelling and simulation of a system of ingestion and excretion of a drug (Fig. 1). The drug is taken orally or in an intravenous way, at a rate $u(t)$, goes to the intestines, where it reaches a quantity $x_1(t)$, and then it is absorbed by the bloodstream with a flow rate $d_1(t)$. The bloodstream, where the drug reaches a quantity $x_2(t)$, passes through the kidney (where it is assumed there is no absorption) with a flow rate $d_2(t)$ that expels the drug at a flow rate $y(t)$, passing it into the urine. In this approach, for reasons of simplicity, other physiological actions are disregarded and the elimination of the drug by cellular metabolism is ignored [5].

In biomedical terminology, this physiological process can be represented by a multi-compartmental process. In this case, if it is assumed that the kidney is only one transition element, the process has two compartments. Being necessary to find a compartmental model of the process, an equivalent fluidic system can be developed, such as that shown in Fig. 2.

Applying the fluidic systems principles, the mass balance of each compartment provides the differential equations for the mathematical model of the overall system. Assuming that $x_1(t)$ and $x_2(t)$ are the corresponding levels (quantities) and the fluidic resistances (R_1 and R_2) are given by:

$$k_1 = \frac{1}{R_1} \ , \ k_2 = \frac{1}{R_2} \tag{1}$$

the following equations are obtained:

$$\begin{gathered} \frac{dx_1(t)}{dt} = -k_1 x_1(t) + k_1 x_2(t) + u(t) \\ \frac{dx_2(t)}{dt} = k_1 x_1(t) - (k_1 + k_2) x_2(t) \\ d_1(t) = k_1 [x_1(t) - x_2(t)] \\ d_2(t) = k_2 x_2(t) \\ y(t) = d_2(t) \end{gathered} \tag{2}$$

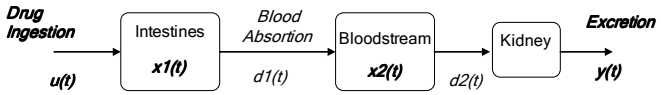

Fig. 1. Diagram of the system of ingestion and excretion of a drug.

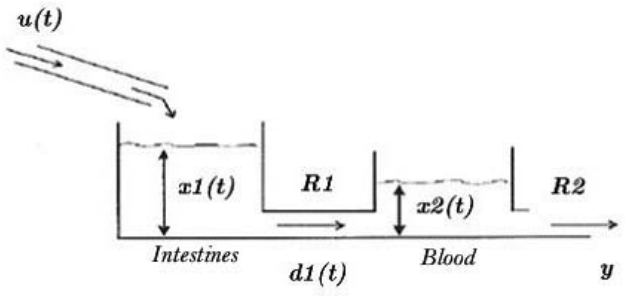

Fig. 2. Fluidic system equivalent to the ingestion and excretion of a drug.

This mathematical model of the ingestion and excretion of a drug can be used for different exercises and experiments as, for example, simulation of the dynamic behaviour of the system, analysis of the system's sensibility to the values of different parameters and design of several types of controllers for a non-linear process.

III. DEMONSTRATION

This work intends to demonstrate the use of a remote and virtual lab that can be used in biomedical engineering courses. In this case, a three-tank system is considered to represent a physiological process, modelling a system of ingestion and excretion of a drug.

Using a Web platform to interact with the remote and virtual lab, students can visualize and obtain data in real time from the remote system. In general terms, the remote experiment can be used for the following purposes: i) identification of the system model; ii) control of the nonlinear system. For the first case, it is possible to send a input signal, $u(t)$, to the remote system and observe and record the resultant response of the system, $y(t)$. For the second situation, the remote system can be controlled considering a local controller with parameters defined by the user or a remote controller interacting in real time with the lab system.

In both cases, before interacting with the remote lab, the students can compare results obtained with a mathematical model simulation and with a virtual representation of the system. Fig. 3 shows the interfaces of the remote (Fig. 3a) and virtual (Fig. 3b) lab using the three-tank system.

The three-tank lab system can also be considered for an improved model of the physiological process, where could be assumed that the kidney is also represented by a compartmental element being $x_3(t)$ the corresponding level (quantity). In this case, the mathematical model should be changed to include a third differential equation to represent the dynamic behaviour of the kidney.

An experimental setup is used to remotely interact with the three-tank system, considering wired communications between the sensors and the micro-computer, acting as server and gateway.

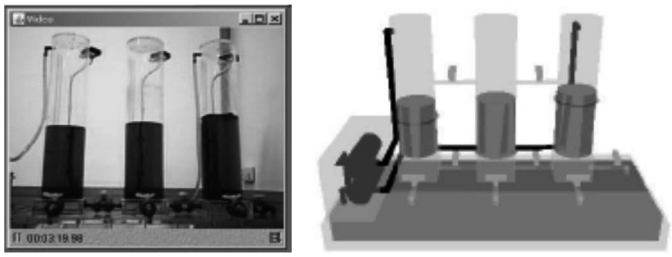

(a) (b)

Fig. 3. Interface of the remote (a) and virtual (b) lab using a three-tank system for the online experiment.

The users can observe the dynamic behaviour of the system through a Web camera. To administrate the access to the remote lab, a management system is provided by the platform, based on a first-come, first-served approach, with the establishment of a maximum threshold for individual usage time.

A Moodle platform is also available with tutorial information, guidelines to carry out the experiments using the experimental setup and quizzes for self-assessment.

IV. CONCLUSION

This work aims to show how a remote and virtual lab can be used to enhance the learning process of students of Biomedical Engineering courses in topics as model identification and control systems.

This demo is an example of online experimentation, where an experimental setup, comprising a three-tank system, is used for modelling and control physiological processes. The interaction trough a Web platform can be done using the remote system or a virtual representation. The developed experiments can be considered in different engineering courses.

ACKNOWLEDGMENT

The authors wish to thank Fundação para a Ciência e a Tecnologia (FCT), CISUC – Centre for Informatics and Systems of the University of Coimbra and iCIS (CENTRO-07-0224-FEDER-002003) for supporting this contribution on online experimentation.

REFERENCES

[1] J. Kretschmer, T. Haunsberger, E. Drost, E. Koch and K. Moller, "Simulating physiological interactions in a hybrid system of mathematical models, Journal of Clinical Monitoring and Computing, 28, 513-523, 2014.

[2] C. Barros, C. P. Leão, F. Soares, G. Minas and J. M. Machado, "RePhyS: a multidisciplinary experience in remote physiological systems laboratory", IJOE, Vol. 9, 2013.

[3] U. Zuperl and M. P. Virtic, "Remote Controlled Laboratory as a Modern Form of Engineering Education", Journal Revija za Elementarno Izobrazevanje, 6 (1), 2013.

[4] A. Valdivieso, M. B. Sánchez, D. Higuita, R. Castelló and M. Villanueva, "Virtual laboratory for simulation and learning of cardiovascular system function in biomedical engineering studies". Rev. Fac. Ing. Univ. Antioquia [online], n.60, pp. 194-201, 2011.

[5] E. N. Bruce, "Biomedical Signal Processing and Signal Modeling". John Wiley and Sons, 2001.